

# Finite-size fluctuations for stochastic coupled oscillators: A general theory

Rupak Majumder<sup>1,\*</sup>, Julien Barré<sup>2,†</sup> and Shamik Gupta<sup>1,‡</sup>

<sup>1</sup>Department of Theoretical Physics, Tata Institute of Fundamental Research, Homi Bhabha Road, Mumbai 400005, India

<sup>2</sup>Institut Denis Poisson, Université d'Orléans, Université de Tours and CNRS, 45067 Orléans, France

Phase transitions, sharp in the thermodynamic limit, get smeared in finite systems where macroscopic order-parameter fluctuations dominate. Achieving a coherent and complete theoretical description of these fluctuations is a central challenge. We develop a general framework to quantify these finite-size effects in synchronization transitions of generic stochastic, globally-coupled nonlinear oscillators. By applying a center-manifold reduction to the nonlinear stochastic PDE for the single-oscillator distribution in finite systems, we derive a mesoscopic description that yields the complete time evolution of the order parameter in the form of a Langevin equation. In particular, this equation provides the first closed-form steady-state distribution of the order parameter, fully capturing finite-size effects. Free from integrability constraints and the celebrated Ott–Antonsen ansatz, our theory shows excellent agreement with simulations across diverse coupling functions and frequency distributions, demonstrating broad applicability. Strikingly, it surpasses recent approaches near criticality and in the incoherent phase, where finite-size fluctuations are most pronounced.

Spontaneous synchronization [1] is a universal phenomenon encountered across disciplines, in physics [2], chemistry [3], biology [4], in systems as diverse as neural networks [5], power grids [6], nanoelectronic platforms [7], flocking animals [8]. Since the seminal work of Winfree and Kuramoto in the 70's [9, 10], globally-coupled populations of nonlinear oscillators have served as paradigmatic models for understanding such a collective behavior. In the infinite-population limit (the thermodynamic limit,  $N \rightarrow \infty$ ), these models often show a phase transition between a synchronized (ordered) and an incoherent (disordered) phase. Theoretical analyses of these models typically consider the thermodynamic limit, where collective dynamics is captured by deterministic mean-field equations for probability distributions over oscillator states [11–15]. This formulation facilitates analytical approaches such as linear stability, bifurcation analysis, and convenient low-dimensional reduction for the time evolution of the synchronization order parameter [16].

In contrast to the infinite-population limit, finite populations exhibit fluctuations in the order parameter. These fluctuations are especially pronounced near the phase transition, where they lead to rounding or smearing of the singularities associated with the transition in the infinite- $N$  limit. Finite- $N$  fluctuations are not captured by theoretical analysis done in the infinite- $N$  limit, underscoring the need for development of analytical tools that account for finite-size effects. This is particularly relevant in light of the fact that real-world systems are inherently finite. Moreover, finite-size effects often have dramatic consequences and can fundamentally alter the system behavior—stabilizing otherwise marginally-unstable unsynchronized states [17], generating output fluctuations (“shot noise”) that shape collective dynamics in neural circuits [18], and producing qualitatively distinct phase transitions in adaptive networks of heterogeneous oscillators [19]. Capturing these effects poses significant analytical challenges. Here, we introduce a general and tractable framework to quantify finite-size effects, and in particular, to characterize how synchronization depends on population size near transition points.

In the thermodynamic limit, the collective dynamics of cou-

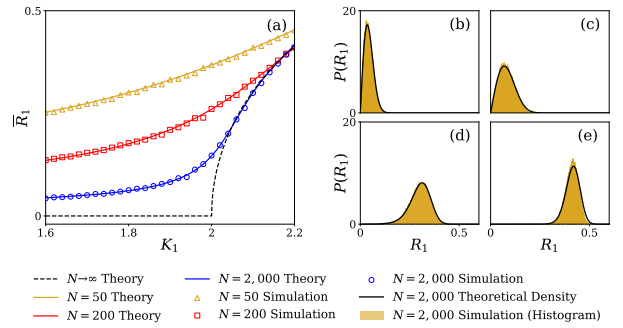


FIG. 1. For model in *Application 1* with  $K_2 = 0$ ,  $D = 1.0$ , the figure shows agreement between our theory (lines) and numerical simulation (markers in (a) and histograms in (b) – (e)) for the average of the steady-state order parameter in (a) and for its distribution in (b) – (e). Parameters for (b) – (e) are  $K_1 = 1.6, 1.9, 2.1, 2.2$ , respectively. Simulation details for all plots are in [20].

pled oscillators is governed by nonlinear integro-differential PDEs for single-oscillator distribution functions. Several foundational approaches have been developed to analyze these equations in Kuramoto-like models, in particular, (i) the self-consistent equation for the order parameter introduced by Kuramoto [10, 21, 22]; (ii) bifurcation theory and center manifold reductions, which are particularly effective near the onset of synchronization [23–31]; and (iii) the Ott–Antonsen (OA) ansatz [16, 32–34], which yields exact low-dimensional reductions even far from criticality, albeit under restrictive conditions. Despite their success in the infinite- $N$  limit, extending these methods to finite populations remains a major challenge. A number of analytical and numerical efforts [35–42] have been initiated to address this issue. Of particular note is the recent work of Ref. [42] for the case of stochastic Kuramoto model, which considers the single-oscillator empirical density that in the limit  $N \rightarrow \infty$  reduces to the single-oscillator distribution function. The work combines (i) the Dean–Kawasaki (DK) equation, a nonlinear stochastic PDE satisfied by the empirical density that captures finite-size fluc-

tuations via multiplicative noise, with (ii) its reduction via the OA ansatz, to derive a single stochastic differential equation for the synchronization order parameter. While powerful, this approach relies on the applicability of the OA ansatz, originally proposed for deterministic dynamics and expected to work only approximately for stochastic dynamics with small noise. Furthermore, the applicability of the ansatz in more complex oscillator models remains to be established.

To address these issues, we propose in this Letter an alternative approach to study finite-size effects in stochastic Kuramoto-like models, by combining two major ingredients: (i) the Dean–Kawasaki equation, and (ii) an extended center manifold expansion near transition points. Our key result is Eq. (5), which gives a single stochastic differential equation for the time evolution of the synchronization order parameter, while taking explicitly into account finite- $N$  effects. This equation is analytically tractable and enables direct access to both static and dynamical properties of the order parameter.

Let us view our approach in the light of Ref. [42] that considers the Kuramoto-Daido order parameters  $Z_m = R_m e^{i\psi_m}$ ;  $m \in \mathbb{Z}^+$ , defined following Eq. (1), and uses the DK equation together with a phase ansatz  $\psi_m = m\psi_1$  to derive a set of coupled evolution equations for the  $R_m$ 's. The evolution of  $R_m$  is coupled to that of  $R_{m-1}$  and  $R_{m+1}$ , and has a drift term  $\propto 1/N$  and a stochastic correlated noise. These coupled equations are (i) used to obtain an approximate expression for average  $R_1$ , the synchronization order parameter, and (ii) numerically solved to obtain the steady-state distribution of  $R_1$ , which are compared with simulations. A remarkable match significantly away from the transition point, even inside the synchronized phase, is reported. The agreement weakens close to the transition, where finite- $N$  fluctuations are most pronounced and which concerns us the most. From the coupled equations of  $R_m$ 's, the OA ansatz yields a closed equation of  $R_1$ , leading to greater disagreement, both at the transition and in the synchronized phase.

In contrast to Ref. [42], our work, which does not rely on the OA ansatz, obtains a closed evolution equation of  $R_1$ , Eq. (5), from which we derive an explicit analytical expression for the full steady-state probability distribution of  $R_1$ , Eqs. (6) and (EM6). This allows to compute the average and in fact any moment of  $R_1$ . Our results thus provide a complete quantitative characterization of finite- $N$  fluctuations in the order parameter, with predictions in excellent agreement with simulations in the incoherent phase and most notably near the transition point, even for  $N$  as small as 50 (see Fig. 1 for the particular model studied in Ref. [42]). Only deep in the synchronized phase, which is beyond the scope of our analysis, does disagreement appear. We extend our study to two more representative cases with increasing complexity and provide excellent agreement with simulations in all cases.

At the heart of our argument lies the observation that in the limit  $N \rightarrow \infty$  and near the phase transition point, the dynamics of the single-oscillator distribution is confined to a center manifold [25], parameterized by the slowest decaying or unstable modes, with the fast decaying modes expressed as

nonlinear functions of the former. Equation (5) relies on the assumption that for large enough but finite  $N$ , the dynamics of the empirical density remains close to the above mentioned center manifold, with finite- $N$  effects making the dynamics on this manifold stochastic. Hence, Eq. (5) is expected to be valid only close to the transition point and for large enough  $N$ , when the noise term in the equation is small. Remarkably, as mentioned above, excellent match with simulations suggests a rather broad range of validity around the transition point and even for small  $N$ . Though not formally rigorous in the mathematical sense, we expect our analysis to be asymptotically exact near transition points, a conjecture supported by rigorous results in related systems [43–45]. Moreover, since the DK equation is related to a large deviation principle for the empirical density [46, 47], our method connects naturally to asymptotic analyses of large deviation principles [48, 49].

Turning to results, we first outline our general strategy and apply it to three increasingly complex variants of the Kuramoto model. Consider a generalized stochastic Kuramoto model of  $N$  globally-coupled limit-cycle oscillators with phases  $\theta_i(t) \in [0, 2\pi)$ ,  $i = 1, 2, \dots, N$ , evolving as

$$\frac{d\theta_i}{dt} = \omega_i + \frac{1}{N} \sum_{j=1}^N f(\theta_j - \theta_i) + \sqrt{2D}\zeta_i(t), \quad (1)$$

with Gaussian, white noise  $\zeta_i(t)$  satisfying  $\langle \zeta_i(t) \rangle = 0$ ,  $\langle \zeta_i(t)\zeta_j(t') \rangle = \delta_{ij}\delta(t-t')$ ,  $D$  denoting noise strength, and quenched-disordered frequencies  $\omega_i$  sampled from distribution  $g(\omega)$ . With inter-oscillator interaction  $f(\theta_j - \theta_i) \forall i, j$  being reciprocal and  $2\pi$ -periodic, we have the Fourier expansion  $f(q) = \sum_{l=1}^{\infty} K_l \sin(lq)$ . This model exhibits phase transitions in the Kuramoto-Daido order parameters  $Z_m(t) = N^{-1} \sum_{j=1}^N e^{im\theta_j(t)}$ ;  $m \in \mathbb{Z}^+$  [50, 51], e.g., Kuramoto model has  $f(q) = K_1 \sin q$ , with order parameter  $R_1 = |Z_1|$  [10].

To describe the dynamics, one usually considers the thermodynamic limit to write a continuity equation for the single oscillator distribution  $F(\theta, \omega, t)$ , which takes the form of a non-linear Fokker-Planck (FP) equation. On the contrary, when  $N$  is finite, the appropriate object of study is the empirical density  $\bar{F}_N(\theta, \omega, t) \equiv N^{-1} \sum_{j=1}^N \delta(\omega - \omega_j) \delta(\theta - \theta_j(t))$ . It is known [52] that this density follows the DK equation:

$$\begin{aligned} \frac{\partial \bar{F}_N(\theta, \omega, t)}{\partial t} = & D \frac{\partial^2 \bar{F}_N(\theta, \omega, t)}{\partial \theta^2} - \frac{\partial}{\partial \theta} [\bar{F}_N(\theta, \omega, t) h] \\ & + \frac{1}{\sqrt{N}} \frac{\partial}{\partial \theta} \left[ \sqrt{2D \bar{F}_N(\theta, \omega, t)} \zeta(\theta, \omega, t) \right]; \quad (2) \end{aligned}$$

$h[\bar{F}_N] \equiv \omega + \int_0^{2\pi} \int_{-\infty}^{\infty} d\theta' d\omega' f(\theta' - \theta) \bar{F}_N(\theta', \omega', t)$  and uncorrelated Gaussian, white noise field  $\zeta(\theta, \omega, t)$  with  $\langle \zeta(\theta, \omega, t) \zeta(\theta', \omega', t') \rangle = \delta(\theta - \theta') \delta(\omega - \omega') \delta(t - t')$ . Equation (2) is to be interpreted in the Itô sense. As  $N \rightarrow \infty$ , when  $\bar{F}_N(\theta, \omega, t) \rightarrow F(\theta, \omega, t)$ , the noise term vanishes and the DK equation reduces to the FP equation for  $F(\theta, \omega, t)$ . We have  $Z_m \equiv R_m e^{im\psi_m} = \int_0^{2\pi} \int_{-\infty}^{\infty} d\theta d\omega e^{im\theta} \bar{F}_N(\theta, \omega, t)$ .

We now focus on bifurcations emerging from the homoge-

neous stationary state, i.e., the incoherent state ( $R_1 = 0$ ). In the incoherent phase, and also near the critical point within the synchronized phase, when the oscillator phases are approximately uniformly distributed over  $[0, 2\pi)$ , we may write  $\bar{F}_N(\theta, \omega, t) = \bar{g}_N(\omega)/(2\pi) + \eta(\theta, \omega, t)$ , where  $\bar{g}_N(\omega)/(2\pi)$  is the finite- $N$  incoherent state and  $\eta$  denotes small fluctuations. Equation (2) accounts for both sources of finite- $N$  fluctuations, due to (i) sampling of the  $N$  frequencies from  $g(\omega)$ , and (ii) the stochastic noise acting on individual oscillators. Since  $\bar{g}_N(\omega)/(2\pi)$  approaches  $g(\omega)/(2\pi)$  at large  $N$ , we replace  $\bar{g}_N$  by  $g$ , thus neglecting fluctuations in frequency sampling for further computations. The DK equation yields

$$\frac{\partial \eta}{\partial t} = \mathcal{L}\eta + \mathcal{N}[\eta] + \sqrt{\frac{2D}{N}} \frac{\partial}{\partial \theta} \left[ \sqrt{\frac{g(\omega)}{2\pi}} + \eta \zeta(\theta, \omega, t) \right]. \quad (3)$$

Here,  $\mathcal{L}$  is a linear and  $\mathcal{N}$  is a nonlinear operator (Appendix A), while the third term arises from the noise field in Eq. (2). With  $\eta(\theta, \omega, t)$  being small,  $\mathcal{L}\eta$  dominates over  $\mathcal{N}[\eta]$ . Furthermore, if  $N$  is sufficiently large such that  $\mathcal{L}\eta$  also dominates over the noise in Eq. (3), the spectrum of  $\mathcal{L}$  governs the leading-order dynamics of  $\eta$ . In the leading order, we may consider the noise term without  $\eta$ , while Appendix E discusses higher-order contributions.

For any function  $\Phi(\theta, \omega)$ , Fourier expansion  $\Phi(\theta, \omega) = \sum_{m=-\infty}^{+\infty} \Phi_m(\omega) e^{im\theta}$  leads to the convenient form  $\mathcal{L}\Phi = \sum_{m=-\infty}^{+\infty} (L_m \Phi_m)(\omega) e^{im\theta}$ . We focus on cases where an instability occurs for modes  $m = \pm 1$ , so that the relevant order parameter is  $Z_1$ . The analysis for any  $m$  follows similarly. Let  $\Psi_m(\theta, \omega) = \psi_m(\omega) e^{im\theta}$  be the most unstable eigenvector of  $L_m$ , with  $\lambda_m$  the corresponding eigenvalue. As system parameters (e.g.,  $K_l$ 's or  $D$  or parameters of  $g(\omega)$ ) are varied,  $\lambda_{\pm 1}$  crossing the imaginary axis implies phase transitions.

As  $N \rightarrow \infty$  and near the transition,  $\eta$  lies on the center manifold, which extends nonlinearly the subspace  $\text{Span}(\Psi_1, \Psi_{-1})$  [23–26, 30], and on which any function  $\mathcal{F}(\theta, \omega, t)$  can be expressed as

$$\mathcal{F}(\theta, \omega, t) = A(t)\Psi_1 + A^*(t)\Psi_{-1} + W[A, A^*], \quad (4)$$

where  $W[A, A^*]$  is the nonlinear contribution, parameterized by the complex number  $A$ , the amplitude along  $\Psi_1$ , and star denotes complex conjugation. Fourier expansion yields  $W[A, A^*] = \sum_{l=-\infty}^{+\infty} W_l e^{il\theta}$ . Exploiting the rotational symmetry of Eq. (1) results in the following structure for the Fourier modes:  $W_0 = 0, W_1 = A|A|^2 h_1(|A|^2), W_l = A^l h_l(|A|^2)$  for  $l = 2, 3, \dots$ , with  $W_{-l} = W_l^*$  [53]. For large enough but finite  $N$ , we now assume the dynamics of  $\eta$  to remain close to the center manifold, allowing  $\eta$  to be expressed in the form (4). Substituting Eq. (4) into Eq. (3), and solving order by order, we obtain a Langevin equation [53]

$$\frac{dA}{dt} = \lambda_1 A - \sum_{n=1}^{\infty} c_{2n+1} A |A|^{2n} + \sqrt{\frac{D_{\text{eff}}}{2\pi^2 N}} \xi(t), \quad (5)$$

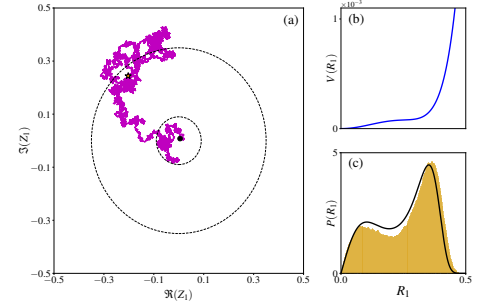


FIG. 2. For model in *Application 1*, the figure shows the behavior near a first-order transition point with  $K_1 = 1.987, K_2 = 2.3, D = 1.0, N = 10^4$ . For the order parameter  $R_1 = |Z_1|$ , panel (a) shows a numerically-obtained trajectory of  $Z_1$  from  $t = 0.0$  (black marker) to  $t = 500.0$  (orange marker), displaying that it jumps between two regions that are close to the maxima of the distribution  $P(R_1)$  and denoted by the two concentric circles. The effective potential  $V(R_1)$  driving the dynamics of  $R_1$  is shown in (b), and agreement between theory (line) and numerical simulation (histogram) is shown in (c).

where we have  $R_1 = 2\pi|A^*[1 + \sum_{n=1}^{+\infty} \mathcal{A}_{1,2n}^* |A|^{2n}]| = 2\pi|A| + \mathcal{O}(|A|^3)$ , and the Gaussian, white noise  $\xi(t) = i\sqrt{2\pi D D_{\text{eff}}^{-1}} \int_{-\infty}^{+\infty} d\omega \int_0^{2\pi} d\theta e^{-i\theta} \tilde{\psi}_1^*(\omega) \sqrt{g(\omega)} \zeta(\theta, \omega, t)$  satisfies  $\langle \xi(t) \rangle = \langle \xi(t) \xi(t') \rangle = 0, \langle \xi(t) \xi^*(t') \rangle = \delta(t - t')$ . The quantities  $\lambda_1, c_{2n+1}, \mathcal{A}_{1,2n}, \tilde{\psi}_1(\omega)$ , effective noise strength  $D_{\text{eff}}$  all depend on system parameters (Appendix B);  $c_{2n+1}$  satisfies a recursion relation, allowing computation for all  $n$ . Although Eq. (5) involves an infinite series, with  $A$  small near transition, a truncated series suffices. With  $A$  complex, Eq. (5) mimics a two-dimensional Brownian motion with a drift.

Equation (5) is the first main result of our work: If the microscopic oscillators are driven by uncorrelated Gaussian, white noise, the order parameter near the transition evolves following Brownian dynamics with a drift. This allows to reduce the  $N$ -body interacting microscopic dynamics to a one-body mesoscopic description, which enables analytical predictions even for finite  $N$ . Notably, finite  $N$  renders the order-parameter dynamics stochastic, with the noise strength scaling as  $1/\sqrt{N}$ . In the thermodynamic limit, when the noise vanishes, the evolution becomes deterministic, recovering all known results [23–26, 30]. Our approach applies to both equilibrium (without frequency disorder) and non-equilibrium systems (with frequency disorder), with Eq. (5) taking the same universal form for both. Our approach differs from phenomenological order parameter evolution in equilibrium systems and near criticality as driven by Landau–Ginzburg free-energy functional [54]; in contrast, we derive the time-evolution equation (5) from microscopic dynamics, with all parameters expressed in terms of microscopic quantities.

From Eq. (5), the condition  $\Re(\lambda_1) = 0$  determines the transition point as  $N \rightarrow \infty$ . The sign of  $\Re(c_3)$  dictates the nature of the transition. For  $\Re(c_3) > 0$ , the transition is continuous, and it suffices to consider terms up to  $\mathcal{O}(|A|^2)$ . For  $\Re(c_3) < 0$ , the transition is first-order, requiring terms at least of  $\mathcal{O}(|A|^4)$ . In the first-order case, the system exhibits two

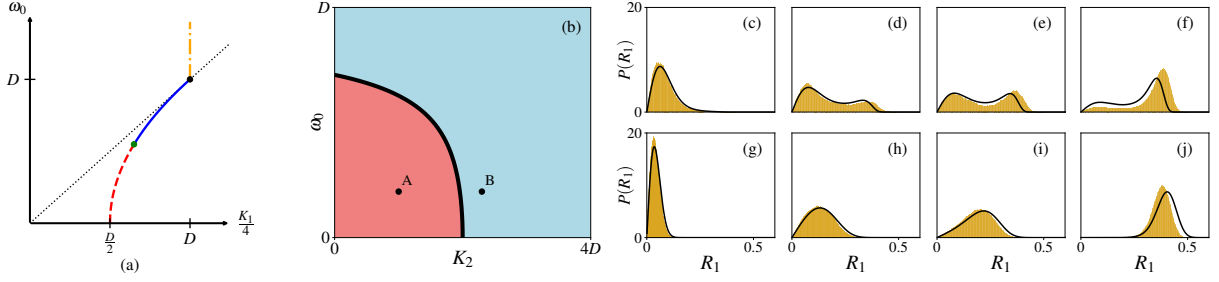


FIG. 3. For model in *Application 2*, (a) shows the  $N \rightarrow \infty$  schematic phase diagram containing the tricritical point (green marker), continuous (red dashed line) and first-order (blue solid line) transition lines for fixed  $K_2$ . (b) Variation of the tricritical point (black line) with  $K_2$ . Upon varying  $K_1$ ,  $R_1$  shows continuous (respectively, first-order) transition for  $(\omega_0, K_2)$  in red-shaded region (e.g.,  $A \equiv (D, 0.2D)$ ) (respectively, blue-shaded region (e.g.,  $B \equiv (2.3D, 0.2D)$ )). For  $D = 1.0$ , agreement between our theory (lines) and numerical simulation (histogram) for first-order transition (point  $B$  with  $K_1 = 2.05, 2.059, 2.0605, 2.063$  and  $N = 10^4$ ) is shown in (c) – (f) and for continuous transition (point  $A$  with  $K_1 = 1.6, 2.059, 2.1, 2.2$  and  $N = 2 \times 10^3$ ) is shown in (g) – (j).

stable states near the transition; as  $N \rightarrow \infty$ , the system settles into one of them depending on the initial condition. However, for finite  $N$ , the Brownian noise in Eq. (5) induces jumps between these states over time, yielding a bimodal steady-state distribution (Fig. 2 and 3(d) – (f)).

When  $\lambda_1$ ,  $D_{\text{eff}}$ , and  $c_{2n+1}$  are real, the deterministic part of Eq. (5) is the derivative of a two-dimensional potential. One then obtains a two-dimensional FP equation for the distribution of  $A$ , giving the steady-state distribution of  $r \equiv |A|$  as

$$\mathbf{P}(r) = \mathcal{M}_0 r e^{-\frac{8\pi^2 N V_0(r)}{D_{\text{eff}}}}; V_0(r) = \sum_{n=0}^{\infty} \frac{c_{2n+1} r^{2(n+1)}}{2(n+1)}, \quad (6)$$

with normalization  $\mathcal{M}_0$  and  $c_1 \equiv -\lambda_1$  [53]. The steady-state distribution  $P(R_1)$  can be obtained numerically from  $\mathbf{P}(r)$  and the change of variable  $R_1(r) = 2\pi r + 2\pi \sum_{n=1}^{\infty} \mathcal{A}_{1,2n} r^{2n+1}$ , when all  $\mathcal{A}_{1,2n}$  are real. An approximate analytical form of  $P(R_1)$  is obtained using  $R_1 \approx 2\pi r$ :  $P_{\approx}(R_1) \sim R_1 \exp[-8\pi^2 N V_0(R_1/2\pi)/D_{\text{eff}}]$ ; it matches very well with  $P(R_1)$  for regions of interest (Appendix C).

This is the second main result of our work: We provide an approximate closed-form expression of the steady-state distribution of  $R_1$  and a closed-form expression of the steady-state distribution of  $|A|$  for finite- $N$  systems. To compute average order parameter in the steady state, we compute the moments  $\overline{r^m} \forall m$  of  $r$  from Eq. (6) and use them to compute  $\bar{R}_1 = \int_0^1 dR_1 R_1 P(R_1) = 2\pi \bar{r} + 2\pi \sum_{n=1}^{\infty} \mathcal{A}_{1,2n} \bar{r}^{2n+1}$ . Having provided all elements of our analysis here and in the Appendices allows to derive explicit results for specific models, which we report below (details in [53]).

*Application 1: Stochastic Kuramoto model with harmonic and bi-harmonic interaction and without frequency:* The first example we consider to showcase our theory is  $g(\omega) = \delta(\omega)$ ,  $f(q) = K_1 \sin q + K_2 \sin 2q$ . With no frequency disorder, finite- $N$  effects arise solely from stochastic noise, and the deterministic part in Eq. (1) writes as the derivative of a potential function, making it an equilibrium model. The operator  $L_m$  has the eigenvalue  $\lambda_m = |m|K_m/2 - m^2 D$  for

$m = \pm 1, \pm 2$ , and  $\lambda_m = -m^2 D$  for  $m = \pm 3, \pm 4, \dots$ . Clearly, for  $K_1 < 2D$  and  $K_2 < 4D$ , all eigenvalues are negative, ensuring the stability of the incoherent phase in the thermodynamic limit. Increasing  $K_1$  while keeping  $K_2 < 4D$  causes  $\lambda_{\pm 1}$  to cross zero at the transition point  $K_1^c = 2D$ , signaling a transition in  $R_1$ . For finite- $N$ , we have Eq. (5) with

$$c_3 = 2\pi^2 K_1 \left( \frac{K_1 - K_2}{K_1 - K_2 + 2D} \right), \quad D_{\text{eff}} = D, \quad (7)$$

with  $c_5$  in [53]. At the transition point,  $c_3 \geq 0$  for  $K_2 \leq 2D$  and  $c_3 < 0$  for  $2D < K_2 \leq 4D$ . Hence, the system undergoes a continuous transition for  $K_2 \leq 2D$  and a first-order transition for  $2D < K_2 < 4D$ . For this model,  $\mathcal{A}_{1,2n} = 0 \forall n \geq 1$  [53], making  $R_1 = 2\pi r$  an exact relation, which gives  $P_{\approx}(R_1) = P(R_1)$ . The very good agreement between our theory and simulations for the continuous transition is shown in Fig. 1 and for the first-order in Fig. 2. Comparison of Eq. (5) with the results in Ref. [42] is given in Appendix E.

*Application 2: Stochastic Kuramoto model with harmonic and bi-harmonic interaction and bi-delta frequency distribution:* The second example we consider is out of equilibrium: we take  $g(\omega) = [\delta(\omega - \omega_0) + \delta(\omega + \omega_0)]/2$ ,  $f(q) = K_1 \sin q + K_2 \sin 2q$ . In the thermodynamic limit, the oscillator population is equally split between frequencies  $+\omega_0$  and  $-\omega_0$ . In this case, one can easily track the frequency-sampling fluctuations: in a particular realization, if  $n$  (respectively,  $N - n$ ) is the number of oscillators with frequency  $+\omega_0$  (respectively,  $-\omega_0$ ), the quantity  $\alpha = n/N$  captures these fluctuations. For this realization,  $\bar{g}_N(\omega) = \alpha \delta(\omega - \omega_0) + (1 - \alpha) \delta(\omega + \omega_0)$ . The operator  $L_m$  has two eigenvalues  $\lambda_{m,\pm} = -m^2 D + (1/4) [K_m \pm \sqrt{(K_m^2 - 16\omega_0^2) + i8(1 - 2\alpha)|m|\omega_0}]$ ;  $m = \pm 1, \pm 2$ , and  $\lambda_{m,\pm} = -m^2 D \pm im\omega_0$  for  $m = \pm 3, \pm 4, \dots$ . The phase diagram of this model in the limit  $N \rightarrow \infty$  is given in Fig. 3(a). Transition points of  $R_1$  are obtained from the condition  $\Re(\lambda_{1,\pm}) = 0$ , which gives  $K_1^c = 2(D + \omega_0^2/D)$  for  $\omega_0 \leq D$  and  $K_1^c = 4D$  for  $\omega_0 > D$ . Note that  $K_1^c$  is independent of  $K_2$ . In the thermodynamic limit, for  $\omega_0 \leq D$ , the



eigenvalues satisfy  $\Re(\lambda_{\pm 1,+}) = 0$  and  $\Re(\lambda_{\pm 1,-}) < 0$  at the transition point. Therefore, the unstable manifold is spanned by only  $\Psi_{\pm 1,+}$ . Our reduced equation (5) thus correctly captures the finite- $N$  effects near the transition in this parameter regime (Red-dashed and blue-continuous line in Fig. 3(a)). A key result is the expression of the effective noise strength  $D_{\text{eff}} \propto [(K_1/4 + \sqrt{(K_1/4)^2 - \omega_0^2})^2 - \omega_0^2]^{-2}$  for  $\alpha = 1/2$ ; its non-trivial dependence on the parameters highlights the need for a theory able to compute it precisely, which our work delivers;  $D_{\text{eff}}$  diverges on  $K_1 = 4\omega_0$  line (black dotted line in Fig. 3(a)), reflecting the fact that on this line, all four eigenvalues  $\lambda_{\pm 1,\pm}$  have the same real part, and a reduced description using only two modes such as in Eq. (4) becomes insufficient. Similarly, for  $\omega_0 > D$ , all four eigenvalues satisfy  $\Re(\lambda_{\pm 1,\pm}) = 0$  at the transition point. As a result, the unstable manifold is spanned by all four eigenfunctions  $\Psi_{\pm 1,\pm}$ . Such higher-dimensional structures can be tackled building on the foundation proposed in the current work. Hence, our analysis is valid on the right of  $K_1 = 4\omega_0$  line, with  $0 \leq \omega_0 < D$ .

As usual, the nature of transition in the limit  $N \rightarrow \infty$  is given by the sign of  $c_3$ , which takes the form  $c_3 \propto [(2D^2 - 4\omega_0^2)(4D^2 + \omega_0^2) - DK_2(4D^2 - 5\omega_0^2)]$ . Comparison between our theory and simulations for the continuous transition is shown in Fig. 3(g) – (j) and for first-order transition in Fig. 3(c) – (f); the agreement is very good close to the transition point and in the incoherent phase, with small discrepancies appearing deep in the synchronized phase.

*Application 3: Stochastic Kuramoto model with harmonic and bi-harmonic interaction and Lorentzian frequency distribution:* The third example we consider has a continuous frequency distribution  $g(\omega) = \sigma [\pi(\omega^2 + \sigma^2)]^{-1}$  and  $f(q) = K_1 \sin q + K_2 \sin 2q$ . The operator  $L_m$  has a continuous spectrum on the line  $\Re(\lambda) = -Dm^2$ , and for  $m = \pm 1, \pm 2$  and  $K_m < 2\sigma$  a single eigenvalue  $\lambda_m = |m|(K_m - 2\sigma)/2 - m^2 D$ . The transition point as  $N \rightarrow \infty$  is  $K_1^c = 2(D + \sigma)$ . For finite- $N$ , we have Eq. (5) with

$$c_3 = \frac{2\pi^2 K_1^2}{K_1 - 2\sigma} \left( \frac{K_1 - K_2 - 2\sigma}{K_1 - K_2 + 2D} \right), \quad D_{\text{eff}} = \frac{DK_1}{K_1 - 2\sigma}, \quad (8)$$

with  $c_5$  in [53];  $\sigma = 0$  in Eq. (8) recovers the expressions in Eq. (7). As noted for *Application II*, the divergence of  $c_3$  and  $D_{\text{eff}}$  at  $K_1 = 2\sigma$  implies the need for a higher-dimensional reduced description, and the above analysis is valid for  $K_1 > 2\sigma$ . Comparison between our theory and simulations is presented in Fig. 5, demonstrating a very good agreement close to the transition and in the incoherent phase.

In summary, our method provides a precise and versatile framework for dealing with finite-size effects in a wide variety of synchronization models. In our treatment, we have not considered frequency-sampling fluctuations, which are discussed in Appendix F. Across all three applications presented, our analysis successfully captures nontrivial finite- $N$  effects in the order parameter distribution, including broad, asymmetric, and bimodal features. Its accuracy within our framework can be systematically improved by increasing the order of the

expansion, or, when necessary, the dimensionality of the reduced description. This paves the way to treating more general models beyond global coupling [55–58], beyond 2D Kuramoto models [59, 60], including for instance non reciprocities [61], as well as more complex dynamical scenarios such as metastability, where finite size effects allow rare transitions between metastable states [28]. From theoretical perspectives, Eq. (5) can be seen as a small-noise SDE, for which there exist powerful techniques of analysis, based on Freidlin-Wentzell large deviation theory and quasi potentials [62, 63]. From experimental perspectives, potential applications lie in optical-cavity setups that inherently deal with a finite number of atoms in optical traps [64–67].

JB thanks R. Chetrite and C. Bernardin for many discussions. This research was supported by Indo-French Centre for the Promotion of Advanced Research (CEFIPRA/IFCPAR) under project identification number 6504-1. S.G. thanks ICTP–Abdus Salam International Centre for Theoretical Physics, Trieste, Italy, for support under its Regular Associateship scheme. We gratefully acknowledge the generous allocation of computing resources by the Department of Theoretical Physics (DTP) of the Tata Institute of Fundamental Research (TIFR), and related technical assistance from Kapil Ghadiali and Ajay Salve. This work is supported by the Department of Atomic Energy, Government of India, under Project Identification Number RTI 4002.

---

\* rupak.majumder@tifr.res.in

† julien.barre@univ-orleans.fr

‡ shamik.gupta@theory.tifr.res.in

- [1] Arkady Pikovsky, Michael Rosenblum, and Jürgen Kurths. Synchronization. Cambridge university press, 12, 2001.
- [2] Kurt Wiesenfeld, Pere Colet, and Steven H. Strogatz. Frequency locking in josephson arrays: Connection with the kuramoto model. *Phys. Rev. E*, 57:1563–1569, Feb 1998.
- [3] Yoshiki Kuramoto and Tomoji Yamada. Pattern formation in oscillatory chemical reactions. *Progress of Theoretical Physics*, 56:724–740, September 1976.
- [4] Renato E. Mirollo and Steven H. Strogatz. Synchronization of pulse-coupled biological oscillators. *SIAM Journal on Applied Mathematics*, 50(6):1645–1662, 1990.
- [5] R. Schmidt, K.J.R. LaFleur, M.A. de Reus, and et al. Kuramoto model simulation of neural hubs and dynamic synchrony in the human cerebral connectome. *BMC Neuroscience*, 16(54), 2015.
- [6] Carl H. Totz, Simona Olmi, and Eckehard Schöll. Control of synchronization in two-layer power grids. *Phys. Rev. E*, 102:022311, Aug 2020.
- [7] Matthew H. Matheny, Jeffrey Emenheiser, Warren Fon, Airle Chapman, Anastasiya Salova, Martin Rohden, Jarvis Li, Mathias Hudoba de Badyn, Márton Pósfai, Leonardo Duenas-Osorio, Mehran Mesbahi, James P. Crutchfield, M. C. Cross, Raissa M. D’Souza, and Michael L. Roukes. Exotic states in a simple network of nanoelectromechanical oscillators. *Science*, 363(6431):eaav7932, 2019.
- [8] Seung-Yeal Ha, Eunhee Jeong, and Moon-Jin Kang. Emergent behaviour of a generalized viscek-type flocking model.

- Nonlinearity*, 23(12):3139, nov 2010.
- [9] Arthur T. Winfree. Biological rhythms and the behavior of populations of coupled oscillators. *Journal of Theoretical Biology*, 16(1):15–42, 1967.
  - [10] Y Kuramoto. *Chemical oscillations, waves, and turbulence*. Springer, 1984.
  - [11] Steven H. Strogatz. From kuramoto to crawford: exploring the onset of synchronization in populations of coupled oscillators. *Physica D: Nonlinear Phenomena*, 143(1):1–20, 2000.
  - [12] Juan A. Acebrón, L. L. Bonilla, Conrad J. Pérez Vicente, Félix Ritort, and Renato Spigler. The kuramoto model: A simple paradigm for synchronization phenomena. *Rev. Mod. Phys.*, 77:137–185, Apr 2005.
  - [13] Shamik Gupta, Alessandro Campa, and Stefano Ruffo. Kuramoto model of synchronization: equilibrium and nonequilibrium aspects. *Journal of Statistical Mechanics: Theory and Experiment*, 2014(8):R08001, Aug 2014.
  - [14] Arkady Pikovsky and Michael Rosenblum. Dynamics of globally coupled oscillators: Progress and perspectives. *Chaos: An Interdisciplinary Journal of Nonlinear Science*, 25(9), 2015.
  - [15] Shamik Gupta, Alessandro Campa, and Stefano Ruffo. *Statistical physics of synchronization*, volume 48. Springer, 2018.
  - [16] Edward Ott and Thomas M Antonsen. Low dimensional behavior of large systems of globally coupled oscillators. *Chaos: An Interdisciplinary Journal of Nonlinear Science*, 18(3):037113, September 2008.
  - [17] Michael A. Buice and Carson C. Chow. Correlations, fluctuations, and stability of a finite-size network of coupled oscillators. *Phys. Rev. E*, 76:031118, Sep 2007.
  - [18] Vladimir V. Klishov and Sergey Yu. Kirillov. Shot noise in next-generation neural mass models for finite-size networks. *Phys. Rev. E*, 106:L062302, Dec 2022.
  - [19] Jan Fialkowski, Serhiy Yanchuk, Igor M. Sokolov, Eckehard Schöll, Georg A. Gottwald, and Rico Berner. Heterogeneous nucleation in finite-size adaptive dynamical networks. *Phys. Rev. Lett.*, 130:067402, Feb 2023.
  - [20] In the simulation the determinatic part is evolved using fourth order Range-Kutta method and the stochastic noise is simulated using Euler–Maruyama method. For  $N = 10000$ , the time step is chosen 0.01 and for  $N = 2000$ , the time step is chosen to be 0.1.
  - [21] Hiroaki Daido. Multibranch entrainment and scaling in large populations of coupled oscillators. *Phys. Rev. Lett.*, 77:1406–1409, Aug 1996.
  - [22] Maxim Komarov and Arkady Pikovsky. Multiplicity of singular synchronous states in the kuramoto model of coupled oscillators. *Phys. Rev. Lett.*, 111:204101, Nov 2013.
  - [23] Steven H Strogatz and Renato E Mirollo. Stability of incoherence in a population of coupled oscillators. *Journal of Statistical Physics*, 63:613–635, 1991.
  - [24] Steven H. Strogatz, Renato E. Mirollo, and Paul C. Matthews. Coupled nonlinear oscillators below the synchronization threshold: Relaxation by generalized landau damping. *Phys. Rev. Lett.*, 68:2730–2733, May 1992.
  - [25] John David Crawford. Amplitude expansions for instabilities in populations of globally-coupled oscillators. *Journal of statistical physics*, 74:1047–1084, 1994.
  - [26] John D. Crawford and K.T.R. Davies. Synchronization of globally coupled phase oscillators: singularities and scaling for general couplings. *Physica D: Nonlinear Phenomena*, 125(1):1–46, 1999.
  - [27] Hayato Chiba. A proof of the kuramoto conjecture for a bifurcation structure of the infinite-dimensional kuramoto model. *Ergodic Theory and Dynamical Systems*, 35(3):762–834, 2015.
  - [28] J. Barré and D. Métivier. Bifurcations and singularities for coupled oscillators with inertia and frustration. *Phys. Rev. Lett.*, 117:214102, November 2016.
  - [29] Hayato Chiba, Georgi S Medvedev, and Matthew S Mizuhara. Bifurcations in the kuramoto model on graphs. *Chaos: an interdisciplinary journal of nonlinear science*, 28(7), 2018.
  - [30] David Métivier and Shamik Gupta. Bifurcations in the time-delayed kuramoto model of coupled oscillators: Exact results. *Journal of Statistical Physics*, 176(2):279–298, 2019.
  - [31] David Métivier, Lucas Wetzel, and Shamik Gupta. Onset of synchronization in networks of second-order kuramoto oscillators with delayed coupling: Exact results and application to phase-locked loops. *Phys. Rev. Res.*, 2:023183, May 2020.
  - [32] Oleh E Omel’chenko. The mathematics behind chimera states. *Nonlinearity*, 31(5):R121, 2018.
  - [33] Irina V. Tyulkina, Denis S. Goldobin, Lyudmila S. Klimenko, and Arkady Pikovsky. Dynamics of noisy oscillator populations beyond the ott-antonsen ansatz. *Phys. Rev. Lett.*, 120:264101, Jun 2018.
  - [34] Christian Bick, Marc Goodfellow, Carlo R Laing, and Erik A Martens. Understanding the dynamics of biological and neural oscillator networks through exact mean-field reductions: a review. *The Journal of Mathematical Neuroscience*, 10(1):9, 2020.
  - [35] Hiroaki Daido. Intrinsic fluctuations and a phase transition in a class of large populations of interacting oscillators. *Journal of Statistical Physics*, 60:753–800, 1990.
  - [36] Oleksandr V. Popovych, Yuri L. Maistrenko, and Peter A. Tass. Phase chaos in coupled oscillators. *Phys. Rev. E*, 71:065201, Jun 2005.
  - [37] Hyunsuk Hong, Hugues Chaté, Hyunggyu Park, and Lei-Han Tang. Entrainment transition in populations of random frequency oscillators. *Phys. Rev. Lett.*, 99:184101, Oct 2007.
  - [38] Hyunsuk Hong, Hugues Chaté, Lei-Han Tang, and Hyunggyu Park. Finite-size scaling, dynamic fluctuations, and hyperscaling relation in the kuramoto model. *Physical Review E*, 92(2):022122, 2015.
  - [39] Maxim Komarov and Arkady Pikovsky. Finite-size-induced transitions to synchrony in oscillator ensembles with nonlinear global coupling. *Phys. Rev. E*, 92:020901, Aug 2015.
  - [40] Franziska Peter and Arkady Pikovsky. Transition to collective oscillations in finite kuramoto ensembles. *Phys. Rev. E*, 97:032310, Mar 2018.
  - [41] Wenqi Yue and Georg A. Gottwald. A stochastic approximation for the finite-size kuramoto–sakaguchi model. *Physica D: Nonlinear Phenomena*, 468:134292, 2024.
  - [42] Víctor Buendía. Mesoscopic theory for coupled stochastic oscillators. *Phys. Rev. Lett.*, 134:197201, May 2025.
  - [43] Francesca Collet and Richard C. Kraaij. Dynamical moderate deviations for the curie–weiss model. *Stochastic Processes and their Applications*, 127(9):2900–2925, 2017.
  - [44] Paolo Dai Pra and Daniele Tovazzi. The dynamics of critical fluctuations in asymmetric curie–weiss models. *Stochastic Processes and their Applications*, 129(3):1060–1095, 2019.
  - [45] Francesca Collet and Paolo Dai Pra. The role of disorder in the dynamics of critical fluctuations of mean field models. *Electronic Journal of Probability*, 17(26):1–40, 2012.
  - [46] Donald A Dawson and Jürgen Gärtner. Large deviations from the mckean-vlasov limit for weakly interacting diffusions. *Stochastics: An International Journal of Probability and Stochastic Processes*, 20(4):247–308, 1987.
  - [47] Paolo Dai Pra and Frank den Hollander. McKean-vlasov limit for interacting random processes in random media. *Journal of*

- statistical physics, 84:735–772, 1996.
- [48] Julien Barré, Cedric Bernardin, Raphaël Chétrite, Yash Chopra, and Mauro Mariani. From fluctuating kinetics to fluctuating hydrodynamics: a  $\gamma$ -convergence of large deviations functionals approach. *Journal of Statistical Physics*, 180(1):1095–1127, 2020.
  - [49] Ouassim Feliachi, Marc Besse, Cesare Nardini, and Julien Barré. Fluctuating kinetic theory and fluctuating hydrodynamics of aligning active particles: the dilute limit. *Journal of Statistical Mechanics: Theory and Experiment*, 2022(11):113207, 2022.
  - [50] Hiroaki Daido. Multibranch entrainment and scaling in large populations of coupled oscillators. *Phys. Rev. Lett.*, 77:1406–1409, Aug 1996.
  - [51] Hiroaki Daido. Onset of cooperative entrainment in limit-cycle oscillators with uniform all-to-all interactions: bifurcation of the order function. *Physica D: Nonlinear Phenomena*, 91(1):24–66, 1996.
  - [52] David S Dean. Langevin equation for the density of a system of interacting langevin processes. *Journal of Physics A: Mathematical and General*, 29(24):L613, 1996.
  - [53] See supplemental material for the derivation of Eqs. (5) and (6) of the main text, all the results for the model in applications 1, 2, and 3, and the derivation of Eq. (13) of the main text.
  - [54] P. C. Hohenberg and B. I. Halperin. Theory of dynamic critical phenomena. *Rev. Mod. Phys.*, 49:435–479, Jul 1977.
  - [55] Georgi S. Medvedev. The continuum limit of the kuramoto model on sparse random graphs. *Communications in Mathematical Sciences*, 17(4):883–898, 2019.
  - [56] Georgi S. Medvedev and Xiaoya Tang. The kuramoto model on power law graphs: Synchronization and contrast states. *Journal of Nonlinear Science*, 30:2405–2427, 2020.
  - [57] Georgi S. Medvedev and Michael S. Mizuhara. Stability of clusters in the second-order kuramoto model on random graphs. *Journal of Statistical Physics*, 182(30), 2021.
  - [58] Paul Dupuis and Georgi S. Medvedev. The large deviation principle for interacting dynamical systems on random graphs. *Communications in Mathematical Physics*, 390:545–575, 2022.
  - [59] Sarthak Chandra, Michelle Girvan, and Edward Ott. Continuous versus discontinuous transitions in the  $d$ -dimensional generalized kuramoto model: Odd  $d$  is different. *Phys. Rev. X*, 9:011002, Jan 2019.
  - [60] Chunming Zheng, Ralf Toenjes, and Arkady Pikovsky. Transition to synchrony in a three-dimensional swarming model with helical trajectories. *Phys. Rev. E*, 104:014216, Jul 2021.
  - [61] Michel Fruchart, Ryo Hanai, Peter B Littlewood, and Vincenzo Vitelli. Non-reciprocal phase transitions. *Nature*, 592(7854):363–369, 2021.
  - [62] Mark Iosifovich Freidlin, Alexander D Wentzell, MI Freidlin, and AD Wentzell. *Random perturbations*. Springer, 1998.
  - [63] Robert Graham. Macroscopic potentials, bifurcations and noise in dissipative systems. In *Fluctuations and Stochastic Phenomena in Condensed Matter: Proceedings of the Sitges Conference on Statistical Mechanics Sitges, Barcelona/Spain, May 26–30, 1986*, pages 1–34. Springer, 2005.
  - [64] Stefan Schütz and Giovanna Morigi. Prethermalization of atoms due to photon-mediated long-range interactions. *Phys. Rev. Lett.*, 113:203002, Nov 2014.
  - [65] Stefan Schütz, Simon B. Jäger, and Giovanna Morigi. Thermodynamics and dynamics of atomic self-organization in an optical cavity. *Phys. Rev. A*, 92:063808, Dec 2015.
  - [66] Simon B. Jäger, Minghui Xu, Stefan Schütz, M. J. Holland, and Giovanna Morigi. Semiclassical theory of synchronization-assisted cooling. *Phys. Rev. A*, 95:063852, Jun 2017.
  - [67] Karl Pelka, Vittorio Peano, and André Xuereb. Chimera states in small optomechanical arrays. *Phys. Rev. Res.*, 2:013201, Feb 2020.
  - [68] Jack Carr. *Applications of Centre Manifold Theory*, volume 35 of *Applied Mathematical Sciences*. Springer, New York, NY, 1 edition, 1981. Springer Book Archive. Springer-Verlag New York Inc. 1982.
  - [69] David Martin, Hugues Chaté, Cesare Nardini, Alexandre Solon, Julien Tailleur, and Frédéric Van Wijland. Fluctuation-induced phase separation in metric and topological models of collective motion. *Physical Review Letters*, 126(14):148001, 2021.

## End Matter

### Appendix A: Expressions of $\mathcal{L}\eta$ and $\mathcal{N}[\eta]$ –

The terms  $\mathcal{L}\eta$  and  $\mathcal{N}[\eta]$  of Eq. (3) read as

$$\mathcal{L}\eta = D \frac{\partial^2 \eta}{\partial \theta^2} - \omega \frac{\partial \eta}{\partial \theta} - \frac{g(\omega)}{2\pi} \times \int_0^{2\pi} d\theta' \int_{-\infty}^{\infty} d\omega' \partial_{\theta} f(\theta' - \theta) \eta(\theta', \omega', t) \quad (\text{EM1})$$

$$\mathcal{N}[\eta] = -\frac{\partial}{\partial \theta} \left[ \eta(\theta, \omega, t) \times \int_0^{2\pi} d\theta' \int_{-\infty}^{\infty} d\omega' f(\theta' - \theta) \eta(\theta', \omega', t) \right] \quad (\text{EM2})$$

### Appendix B: Expressions of $\lambda_1$ , $c_{2n+1}$ , $D_{\text{eff}}$ (for derivation, see [53]) –

Let  $\Psi_1(\theta, \omega) = \psi_1(\omega) e^{i\theta}$  be the eigenfunction of  $\mathcal{L}$  with eigenvalue  $\lambda_1$ , given by the root of the function  $\Lambda_1(x)$  defined as  $\Lambda_1(x) \equiv 1 - (K_1/2) \int_{-\infty}^{\infty} d\omega g(\omega) / (x + D + i\omega)$ , where we have  $\psi_1(\omega) = K_1 g(\omega) / [2(\lambda_1 + D + i\omega)]$ . Similarly,  $\tilde{\Psi}_1(\theta, \omega) = (2\pi)^{-1} \tilde{\psi}_1(\omega) e^{i\theta}$  is the eigenfunction of  $\mathcal{L}^\dagger$  with eigenvalue  $\lambda_1^*$ , with  $\tilde{\psi}_1(\omega) = [[\Lambda_1'(\lambda_1)]^* (\lambda_1^* + D - i\omega)]^{-1}$ . The effective noise strength is given by

$$D_{\text{eff}} = D \int_{-\infty}^{+\infty} d\omega \left| \tilde{\psi}_1(\omega') \right|^2 g(\omega). \quad (\text{EM3})$$

The expression for the coefficients  $c_{2n+1}$  is given by

$$c_{2n+1} = \pi \sum_{l=1}^{\infty} K_l \sum_{q=0}^{n-l+1} \left[ \mathcal{B}_{l+1,2q} \mathcal{A}_{l,2(n-l-q)}^* \Theta(n-l-q) - \mathcal{C}_{l-1,2q}^* \mathcal{A}_{l,2(n-l+1-q)} \right], \quad (\text{EM4})$$

for  $n = 1, 2, \dots$  and  $\Theta(x) = 1 \forall x \geq 0$  and  $\Theta(x) = 0 \forall x < 0$ . Here, we have  $\mathcal{A}_{m,2p} \equiv \int_{-\infty}^{\infty} d\omega w_{m,2p}$ ,  $\mathcal{B}_{m,2p} \equiv \int_{-\infty}^{\infty} d\omega \tilde{\psi}_1^* w_{m,2p}$ ,  $\mathcal{C}_{m,2p} \equiv \int_{-\infty}^{\infty} d\omega \tilde{\psi}_1 w_{m,2p}$  with  $c_1 \equiv -\lambda_1$ ,  $w_{0,2p} = 0 \forall p$ ,  $w_{1,0} \equiv \psi_1$ , while for  $m > 0$ , we have

$$w_{m,2p} = \left[ \frac{1}{(m+p)\lambda_1 + p\lambda_1^* + m^2 D + im\omega} \right] \times \left[ \sum_{q=0}^{p-1} \left[ (m+q)c_{2(p-q)+1} + q\mathcal{C}_{2(p-q)+1}^* \right] w_{m,2q} + m\pi \sum_{l=1}^m K_l \sum_{q=0}^p w_{m-l,2q} \mathcal{A}_{l,2(p-q)} + m\pi \sum_{l=m+1}^{\infty} K_l \sum_{q=0}^{m+p-l} w_{l-m,2q}^* \mathcal{A}_{l,2(m+p-l-q)} - m\pi \sum_{l=1}^{\infty} K_l \sum_{q=0}^{p-l} w_{m+l,2q} \mathcal{A}_{l,2(p-l-q)} + \frac{mK_m}{2} g(\omega) \mathcal{A}_{m,2p} \right]. \quad (\text{EM5})$$

### Appendix C: Comparison between $P(R_1)$ and $P_{\approx}(R_1)$ –

From the expansion  $R_1(r) = 2\pi r + 2\pi \sum_{n=1}^{\infty} \mathcal{A}_{1,2n} r^{2n+1}$ , approximating  $R_1$  as  $R_1 \approx 2\pi r$ , we obtain an approximate analytical expression of  $P(R_1) = \mathbf{P}(r)/(dR_1/dr)$  may be obtained as  $P_{\approx}(R_1) = \mathbf{P}(R_1/(2\pi))/(2\pi)$ , which on using Eq. (6) reads as

$$P_{\approx}(R_1) = \mathcal{M} R_1 e^{-\frac{2NV(R_1)}{D_{\text{eff}}}}; \quad V(R_1) = \sum_{n=0}^{\infty} \frac{c_{2n+1} R_1^{2(n+1)}}{2(n+1)(2\pi)^{2n}}. \quad (\text{EM6})$$

In general,  $P_{\approx}(R_1)$  could deviate from  $P(R_1)$ . Remarkably, near the phase transition, which is also our region of interest,  $P_{\approx}(R_1)$  and  $P(R_1)$  agree quite well (Fig. 4).

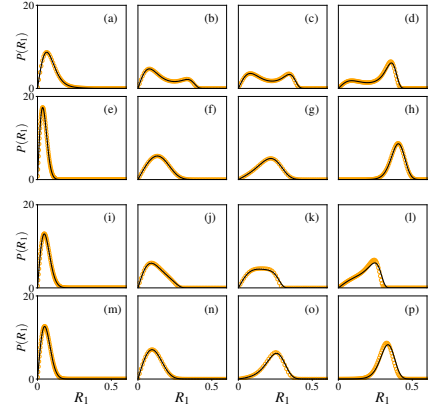


FIG. 4. Agreement between  $P_{\approx}(R_1)$  (line) and  $P(R_1)$  (unfilled markers) for the model in *Application 2* ((a) – (h)) and the one in *Application 3* ((i) – (p)) is shown. Parameters for (a) – (h) are the same as in Fig. 3, panels (c) – (j), respectively. Similarly, parameters for (i) – (p) are the same as in Fig. 5, panels (c) – (j), respectively.

### Appendix D: Application 1, effective SDE for $R_1$

The model studied in Ref. [42] is the model considered in *Application 1* of our Letter for the particular case  $K_2 = 0$ . Putting  $K_2 = 0$  in Eq. (7), we obtain from Eq. (5) by retaining terms up to  $\mathcal{O}(|A|^2)$  that

$$\frac{dA}{dt} = \left[ \frac{K_2}{2} - D \right] A - \left[ \frac{2\pi^2 K_1^2}{K_1 + 2D} \right] A |A|^2 + \sqrt{\frac{D}{2\pi^2 N}} \xi(t). \quad (\text{EM7})$$

As discussed in the main text, for this model, we have  $R_1 = 2\pi |A|$ . Noting that  $R_1 = 2\pi \sqrt{A A^*}$ , and using Taylor expansion of  $R_1$  up to second order and the Itô calculus, we obtain the evolution of  $R_1$  from Eq. (EM7) as

$$\frac{dR_1}{dt} = \left[ \frac{K_1}{2} - D \right] R_1 - \frac{1}{2} \left[ \frac{K_1^2}{K_1 + 2D} \right] R_1^3 + \frac{D}{NR_1} + \sqrt{\frac{D}{N}} \xi_r(t), \quad (\text{EM8})$$

with  $\langle \xi_r(t) \rangle = 0$  and  $\langle \xi_r(t) \xi_r(t') \rangle = \delta(t - t')$ . If we had retained the  $\eta$  term in the noise appearing in Eq. (3) (see the



main text following Eq. (3)), Eq. (EM8) would be modified to [53]

$$\begin{aligned} \frac{dR_1}{dt} = & \left[ \frac{K_1}{2} - D \right] R_1 - \frac{1}{2} \left[ \frac{K_1^2}{K_1 + 2D} \right] R_1^3 \\ & + \frac{D}{NR_1} \left[ 1 + R_1^2 \left( \frac{K_1}{K_1 + 2D} \right) \right] \\ & + \sqrt{\frac{D}{N}} \left[ 1 - R_1^2 \left( \frac{K_1}{K_1 + 2D} \right) \right] \xi_r(t). \end{aligned} \quad (\text{EM9})$$

We compare Eq. (EM9) with Eq. (11) of Ref. [42], which reads as

$$\begin{aligned} \frac{dR_1}{dt} = & \left[ \frac{K_1}{2} - D \right] R_1 - \frac{K_1}{2} R_1^3 + \frac{D[1 + R_1^2]}{NR_1} \\ & + \sqrt{\frac{D[1 - R_1^2]}{N}} \xi_r(t). \end{aligned} \quad (\text{EM10})$$

We observe that the coefficient of  $R_1^3$  in the two equations does not match. Moreover, inside the brackets of the third and fourth terms on the right hand side, the coefficient of  $R_1^2$  does not match. These terms come from the part of  $\eta(\theta, \omega, t)$  that nonlinearly depends on  $A(t)$  (see the discussions before Eq. (4)), which in turn originate from the nonlinear  $\eta$  contributions in Eq. (3). Reference [42] used the OA ansatz to deal with these nonlinear  $\eta$  contributions, whereas we use center manifold expansion, which is the reason for the mismatch in the corresponding coefficients. Since a center manifold expansion is asymptotically exact near the transition point [68], our method captures finite- $N$  fluctuations extremely well near the transition point, as compared to Ref. [42].

Equation (EM10) agrees with Eq. (EM9) in two limits: (i) When  $R_1$  is small, both equations reduce to  $dR_1/dt = [K_1/2 - D] R_1 + D/(NR_1) + \sqrt{D/N} \xi_r(t)$ . For  $K_1 < 2D$  (incoherent phase), when  $R_1$  is small, both the equations describe well finite-size fluctuations in the incoherent phase. (ii) The other limit when Eq. (EM9) reduces to Eq. (EM10) is when  $K_1 \gg D$ , enabling us to have  $K_1 + 2D \approx K_1$ . Hence, Eq. (EM10) agrees with Eq. (EM9) when the noise strength  $D$  is very small. This reflects the fact that the OA ansatz, on which the analysis in Ref. [42] was based, was proposed for the noiseless Kuramoto model, and only works approximately for very small noise strength. Near the transition point ( $K_1 = 2D$ ), when both  $K_1$  and  $D$  are of same order, the agreement of Ref. [42] with simulations suffers.

#### Appendix E: Results for Application 3

The results are shown in Fig. 5.

#### Appendix F: Fluctuations in $g(\omega)$ –

For *Application II* we considered the frequency-sampling fluctuations by introducing the parameter  $\alpha$  (*Application I* has no frequency disorder). However, for *Application III* involving the heavy-tailed Lorentzian distribution, Fig. 6 shows that for small  $N$ , sample-to-sample fluctuations of  $\bar{g}_N(\omega)$  induce visible deviations in the corresponding steady-state histogram

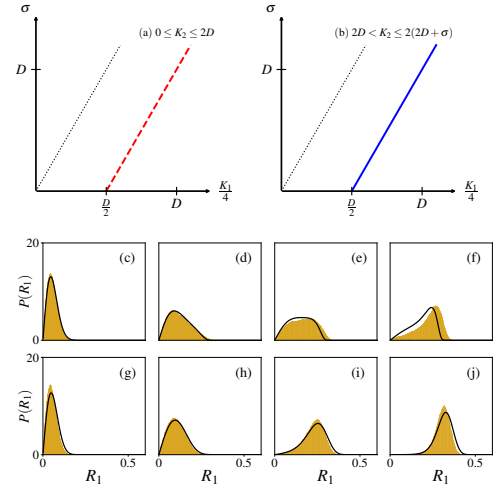


FIG. 5. For model in *Application 3*, (a) and (b) show the  $N \rightarrow \infty$  phase diagram containing the continuous (red dashed line) and first-order (blue solid line) transition lines in the  $\sigma - K_1$  plane for fixed  $K_2$ . For  $\sigma = 1.0, D = 1$ , agreement between our theory (lines) and numerical simulation (histogram) for first-order transition ( $K_2 = 2.3$  with  $K_1 = 3.9, 3.97, 3.98, 3.99$  and  $N = 10^4$ ) is shown is (c) – (f) and for continuous transition ( $K_2 = 1.0$  with  $K_1 = 3.5, 3.9, 4.1, 4.2$  and  $N = 2 \times 10^3$ ) is shown is (g) – (j).

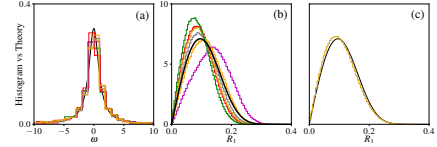


FIG. 6. For *Application III* with  $K_1 = 3.9, K_2 = 1.0, D = 1.0, \sigma = 1.0, N = 2000$ : (a) frequency histograms  $\bar{g}_N(\omega)$  from different realizations of sampled frequencies (colored) compared with the Lorentzian  $g(\omega)$  (black). These are obtained for typical realizations of the frequencies, where for each oscillator, its frequency is sampled independently from the distribution  $g(\omega)$ . (b) Steady-state histograms of  $R_1$  for the corresponding samples (colored), with the theoretical  $P(R_1)$  shown in black. (c) Agreement between the average (colored) of the six histograms presented in (b) and  $P(R_1)$  (black).

of  $R_1$  with respect to the distribution of  $P(R_1)$  predicted theoretically by replacing  $\bar{g}_N(\omega)$  by  $g(\omega)$ . Nevertheless, averaging these histograms over different frequency realizations gives excellent agreement with  $P(R_1)$ , demonstrating that our theory captures the mesoscopic fluctuations due to dynamical Gaussian noise, but not the quenched ones, arising from frequency sampling at small  $N$ . A possible remedy to access the quenched fluctuations is to approximate a given realization  $\bar{g}_N(\omega) = N^{-1} \sum_{j=1}^N \delta(\omega - \omega_j)$  by coarse-graining it into  $M$  bins within  $[-\Omega, \Omega]$ , and approximating it as  $\bar{g}_N(\omega) \approx (\sum_{m=0}^{M-1} f_m)^{-1} \sum_{m=0}^{M-1} f_m \delta[\omega - \Omega(2m+1-M)/M]$ , where  $f_m$  is the number of sampled frequencies in the  $m$ -th bin. This amounts to a generalization of our analysis, which we leave for future work.

**Supplementary Information for: “Finite-size fluctuations for stochastic coupled oscillators: A general theory”**

**CONTENTS**

References	5
A. Derivation of Eq. (5) of the main text	10
B. Derivation of Eq. (6) of the main text	17
C. Results corresponding to the model in <i>Application 1</i> of the main text	17
D. Results corresponding to the model in <i>Application 2</i> of the main text	20
E. Results corresponding to the model in <i>Application 3</i> of the main text	23
F. Derivation of Eq. (13)	24

**Appendix A: Derivation of Eq. (5) of the main text**

We start with the global noise field  $\zeta(\theta, \omega, t)$  in Eq. (2) of the main text. Since  $\zeta(\theta, \omega, t)$  is  $2\pi$ -periodic in  $\theta$ , we can express it in a Fourier series as  $\zeta(\theta, \omega, t) = \sum_{l=-\infty}^{+\infty} \xi_l(\omega, t) e^{il\theta}$ . The properties of  $\zeta(\theta, \omega, t)$  given by  $\langle \zeta(\theta, \omega, t) \rangle = 0$  and  $\langle \zeta(\theta, \omega, t) \zeta(\theta', \omega', t') \rangle = \delta(\theta - \theta') \delta(\omega - \omega') \delta(t - t')$  put further conditions on the Fourier coefficients as

$$\langle \xi_l(\omega, t) \rangle = \langle \xi_l(\omega, t) \xi_m(\omega', t') \rangle = 0, \quad (\text{SM1})$$

$$\langle \xi_l(\omega, t) \xi_m^*(\omega', t') \rangle = \frac{1}{2\pi} \delta_{lm} \delta(\omega - \omega') \delta(t - t'). \quad (\text{SM2})$$

These relations will be useful later.

For further computations, we are interested in the bifurcations from the homogeneous stationary state, i.e., the incoherent state. In this parameter region with  $N \rightarrow \infty$ , the density is simply  $\bar{F}_{N \rightarrow \infty}(\theta, \omega, t \rightarrow \infty) = g(\omega)/(2\pi)$ , where  $g(\omega)$  is the distribution function of the frequencies. When  $N$  is finite, we shall assume that it is large enough so that  $\bar{g}_N$  can be replaced by  $g$ . We can then express the finite- $N$  empirical density in the following form:

$$\bar{F}_N(\theta, \omega, t) = \frac{g(\omega)}{2\pi} + \eta(\theta, \omega, t), \quad (\text{SM3})$$

where  $\eta(\theta, \omega, t)$  is small.

Putting Eq. (SM3) into Eq. (2) of the main text, we obtain

$$\frac{\partial \eta}{\partial t} = \mathcal{L}\eta + \mathcal{N}[\eta] + \sqrt{\frac{2D}{N}} \frac{\partial}{\partial \theta} \left[ \sqrt{\frac{g(\omega)}{2\pi}} + \eta \zeta(\theta, \omega, t) \right], \quad (\text{SM4})$$

where  $\mathcal{L}$  is a linear operator and  $\mathcal{N}$  is a non-linear operator, which read as

$$\mathcal{L}\eta = D \frac{\partial^2 \eta}{\partial \theta^2} - \omega \frac{\partial \eta}{\partial \theta} - \frac{g(\omega)}{2\pi} \int_0^{2\pi} d\theta' \int_{-\infty}^{\infty} d\omega' \partial_\theta f(\theta' - \theta) \eta(\theta', \omega', t), \quad (\text{SM5})$$

$$\mathcal{N}[\eta] = -\partial_\theta \left[ \eta(\theta, \omega, t) \int_0^{2\pi} d\theta' \int_{-\infty}^{\infty} d\omega' f(\theta' - \theta) \eta(\theta', \omega', t) \right]. \quad (\text{SM6})$$

As mentioned in the main text, in the leading order, we may consider the noise term without  $\eta$  for further computations, which gives us

$$\frac{\partial \eta}{\partial t} = \mathcal{L}\eta + \mathcal{N}[\eta] + \sqrt{\frac{Dg(\omega)}{\pi N}} \frac{\partial}{\partial \theta} \left[ \zeta(\theta, \omega, t) \right]. \quad (\text{SM7})$$

In Eq. (SM7), we have kept only the leading order of the noise, which makes the noise term in the equation, which was otherwise multiplicative, to be additive, see Ref. [69] for an example where the multiplicative structure is qualitatively important. With  $\eta(\theta, \omega, t)$  being small,  $\mathcal{L}\eta$  dominates over  $\mathcal{N}[\eta]$ . Furthermore,  $N$  is sufficiently large such that  $\mathcal{L}\eta$  also dominates over the noise in Eq. (SM7). Hence, at leading order, the dynamics of  $\eta$  will be determined by the operator  $\mathcal{L}$ .

Before moving forward, let us understand the action of operators  $\mathcal{L}$  and  $\mathcal{N}$  in detail. Let  $\Phi \equiv \Phi(\theta, \omega)$  be a general function. The angle  $\theta$  being  $2\pi$ -periodic, we can use the following Fourier expansions:  $\Phi(\theta, \omega) = \sum_{m=-\infty}^{+\infty} \Phi_m(\omega) e^{im\theta}$ ,  $\mathcal{L}\Phi = \sum_{m=-\infty}^{+\infty} (L_m \Phi_m) e^{im\theta}$ , and  $\mathcal{N}[\Phi] = \sum_{m=-\infty}^{+\infty} \mathcal{N}_m[\Phi] e^{im\theta}$ . Furthermore, we have  $f(q) = \sum_{l=1}^{+\infty} K_l \sin(lq)$ . Putting these expansions back into Eq. (SM5) and comparing the Fourier modes of both sides, we obtain

$$L_m \Phi_m = -(m^2 D + im\omega) \Phi_m(\omega) + \frac{g(\omega)}{2} \int_{-\infty}^{\infty} d\omega' \Phi_m(\omega') \sum_{l=1}^{+\infty} l K_l (\delta_{l,m} + \delta_{l,-m}), \quad (\text{SM8})$$

where  $\delta_{a,b}$ 's are Kronecker deltas. Similarly, putting the Fourier expansions back into Eq. (SM6), we obtain

$$\mathcal{N}_m[\Phi] = \pi m \sum_{l=1}^{+\infty} K_l \left[ \Phi_{m-l}(\omega) \int_{-\infty}^{+\infty} d\omega' \Phi_l(\omega') - \Phi_{m+l}(\omega) \int_{-\infty}^{+\infty} d\omega' \Phi_{-l}(\omega') \right]. \quad (\text{SM9})$$

We now focus on finding the spectrum of the linear operator  $\mathcal{L}$ ; for more details, see [25]. Considering  $\Psi_m(\theta, \omega) = \psi_m(\omega) e^{im\theta}$  to be its eigenfunction with the eigenvalue  $\lambda_m$ , the eigenvalue equation  $\mathcal{L}\Psi_m = \lambda_m \Psi_m$  gives  $L_m \psi_m = \lambda_m \psi_m$ . Using Eq. (SM8), we obtain

$$(\lambda_m + m^2 D + im\omega) \psi_m(\omega) = \frac{|m| K_{|m|} g(\omega)}{2} \int_{-\infty}^{\infty} d\omega' \psi_m(\omega'). \quad (\text{SM10})$$

For any  $m$  such that  $K_{|m|} = 0$ , the only possible functions  $\psi_m$  are singular, corresponding to the existence of a continuous spectrum on the line  $\text{Re}(\lambda) = -Dm^2$ . For  $m$  such that  $K_{|m|} \neq 0$ , there is still a continuous spectrum on the line  $\text{Re}(\lambda) = -Dm^2$ , but there may also exist nonsingular solutions to (SM10), corresponding to the discrete spectrum which will be our main interest. They satisfy:

$$\psi_m(\omega) = \frac{|m| K_{|m|} g(\omega)}{2(\lambda_m + m^2 D + im\omega)} \int_{-\infty}^{\infty} d\omega' \psi_m(\omega'). \quad (\text{SM11})$$

Integrating both sides of Eq. (SM11) with respect to  $\omega$  and noting that  $\int_{-\infty}^{\infty} d\omega' \psi_m(\omega') \neq 0$ , we obtain the secular equation determining the eigenvalues, which reads as  $\Lambda_m(\lambda_m) = 0$ , where  $\Lambda_m$  is the spectral function

$$\Lambda_m(x) = 1 - \frac{|m| K_{|m|}}{2} \int_{-\infty}^{\infty} d\omega' \frac{g(\omega')}{(x + m^2 D + im\omega')}. \quad (\text{SM12})$$

Interestingly, the spectral function satisfies the identity  $[\Lambda_m(x)]^* = \Lambda_{-m}(x^*)$ , with the star denoting complex conjugation. Hence, if  $\lambda_m$  is a root of  $\Lambda_m(x)$ , then  $\lambda_m^*$  is also a root of  $\Lambda_{-m}(x)$ . Clearly, the eigenvalues  $\lambda_m$  change upon changing the interaction strength  $K_{|m|}$  of the corresponding Fourier mode. Using the normalization  $\int_{-\infty}^{\infty} d\omega' \psi_m(\omega') = 1$ , we can write

$$\psi_m(\omega) = \frac{|m| K_{|m|} g(\omega)}{2(\lambda_m + m^2 D + im\omega)}. \quad (\text{SM13})$$

We may further define an adjoint operator for the linear operator  $\mathcal{L}$  from the definition  $(A, \mathcal{L}B) = (\mathcal{L}^\dagger A, B)$ , where the inner product is given by  $(A, B) = \int_0^{2\pi} d\theta \int_{-\infty}^{+\infty} d\omega' A^*(\theta', \omega') B(\theta', \omega')$ . Defining the Fourier expansions  $A(\theta, \omega) \equiv (2\pi)^{-1} \sum_{m=-\infty}^{+\infty} A_m(\omega) e^{im\theta}$  and  $\mathcal{L}^\dagger A \equiv (2\pi)^{-1} \sum_{m=-\infty}^{+\infty} (L_m^\dagger A_m) e^{im\theta}$  and using the definition of  $\mathcal{L}^\dagger$  along with Eq. (SM8), we obtain

$$L_m^\dagger A_m = -(m^2 D - im\omega) A_m(\omega) + \frac{1}{2} \int_{-\infty}^{\infty} d\omega' g(\omega') A_m(\omega') \sum_{l=1}^{+\infty} l K_l (\delta_{l,m} + \delta_{l,-m}). \quad (\text{SM14})$$

The spectrum of  $\mathcal{L}^\dagger$  may be found in the following way. Considering  $\tilde{\Psi}_m(\theta, \omega) = (2\pi)^{-1} \tilde{\psi}_m(\omega) e^{im\theta}$  to be its eigenfunction

with the eigenvalue  $\lambda_{\dagger,m}$ , the eigenvalue equation  $\mathcal{L}^\dagger \tilde{\Psi}_m = \lambda_{\dagger,m} \tilde{\Psi}_m$  gives  $L_m^\dagger \tilde{\psi}_m = \lambda_{\dagger,m} \tilde{\psi}_m$ . Using Eq. (SM14), we obtain

$$(\lambda_{\dagger,m} + m^2 D - im\omega) \tilde{\psi}_m(\omega) = \frac{|m|K_{|m|}}{2} \int_{-\infty}^{\infty} d\omega' g(\omega') \tilde{\psi}_m(\omega'). \quad (\text{SM15})$$

Similar to the case of  $\mathcal{L}$ , if there exists an  $m$  such that  $K_{|m|} = 0$ , then we have the trivial solution  $\lambda_{\dagger,m} = -m^2 D + im\omega$  with  $\tilde{\psi}_m(\omega') = \delta(\omega' - \omega)$ . On the contrary, if  $K_{|m|} \neq 0$ , we have the nontrivial solution

$$\tilde{\psi}_m(\omega) = \frac{|m|K_{|m|}}{2(\lambda_{\dagger,m} + m^2 D - im\omega)} \int_{-\infty}^{\infty} d\omega' g(\omega') \tilde{\psi}_m(\omega'). \quad (\text{SM16})$$

Multiplying both sides of Eq. (SM16) by  $g(\omega)$  and integrating with respect to frequency, we obtain that the eigenvalue  $\lambda_{\dagger,m}$  of the operator  $\mathcal{L}^\dagger$  is the root of the spectral function

$$\Lambda_{\dagger,m}(x) = 1 - \frac{|m|K_{|m|}}{2} \int_{-\infty}^{\infty} d\omega' \frac{g(\omega')}{(x + m^2 D - im\omega')}. \quad (\text{SM17})$$

Comparing Eqs. (SM12) and (SM17), we obtain  $\Lambda_{\dagger,m}(x) = \Lambda_{-m}(x)$ . Hence, the eigenvalues of  $\mathcal{L}^\dagger$  corresponding to  $m$ -th Fourier mode are exactly the same as the eigenvalues of  $\mathcal{L}$  corresponding to  $(-m)$ -th Fourier mode. These in turn are the same as the complex conjugates of the eigenvalues of  $\mathcal{L}$  corresponding to  $m$ -th Fourier mode. Mathematically,  $\lambda_{\dagger,m} = \lambda_{-m} = \lambda_m^*$ . Furthermore, imposing the orthonormality condition  $(\tilde{\Psi}_m, \Psi_{m'}) = \delta_{m,m'}$  gives

$$\tilde{\psi}_m(\omega) = \frac{1}{[\Lambda'_m(\lambda_m)]^*} \frac{1}{(\lambda_{\dagger,m} + m^2 D - im\omega)}. \quad (\text{SM18})$$

In the incoherent phase, the real part of all the eigenvalues are negative, i.e.,  $\Re(\lambda_m) < 0$ . Hence, any perturbation of the incoherent state will die down fast in time, making it a stable state. Upon changing  $K_{|m|}$  for a particular  $m$ , keeping all other interaction strengths constant, it may so happen that once  $K_{|m|}$  crosses a particular value, say  $K_{|m|}^c$ ,  $\Re(\lambda_m)$  and  $\Re(\lambda_{-m})$  for that particular  $m$  change sign and become positive. As a result, any perturbation along the direction of  $\Psi_m(\theta, \omega)$  and  $\Psi_{-m}(\theta, \omega)$  will grow with time, making the incoherent phase unstable. At linear order in the perturbation, the dynamics is then confined to the linear subspace  $\text{Span}(\Psi_m, \Psi_{-m})$ . In the deterministic case (i.e., without noise) and close to the bifurcation/transition, the nonlinearities drive the dynamics outside  $\text{Span}(\Psi_m, \Psi_{-m})$ ; however, it remains confined to a manifold (the center manifold), which is a nonlinear deformation of  $\text{Span}(\Psi_m, \Psi_{-m})$ . The goal of the (deterministic) center manifold expansion is to determine at the same time this manifold and the slow dynamics that takes place on it (see Refs. [23–26, 30, 31] for implementations in the context of synchronization models in the thermodynamic limit). Our crucial hypothesis is that the finite- $N$  noise will not drive the system too far from the deterministic center manifold, so that we only have to understand how the noise impacts the dynamics on the center manifold. Similar effect will also be there when  $\Re(\lambda_{\pm m})$  is least negative among the rest of the eigenvalues. In this case also, there will be a timescale separation of the dynamics of  $\eta(\theta, \omega, t)$  on the subspace  $\text{Span}(\Psi_m, \Psi_{-m})$  and orthogonal to it, resulting in a net dynamics of  $\eta(\theta, \omega, t)$  on the center manifold.

For the next part of the calculation, we will assume that  $K_1$  is varied keeping all the other  $K_{|m|}$ 's fixed. Hence,  $\Re(\lambda_{\pm 1})$  changes sign, while all other  $m$ 's have  $\Re(\lambda_m) < 0$ . As a result, the Kuramoto-Daido order parameter  $R_1$  shows a phase transition. This calculation may be reproduced for any other order parameter  $R_m$  showing a phase transition.

Since,  $\Re(\lambda_{\pm 1})$  is changing sign, let us assume that we are at a parameter region such that  $\Re(\lambda_{\pm 1})$  is either positive or least negative among all other  $\Re(\lambda_m)$ . Hence, following the previous discussion, we may write

$$\eta(\theta, \omega, t) = A(t)\Psi_1(\theta, \omega) + A^*(t)\Psi_{-1}(\theta, \omega) + S(\theta, \omega, t). \quad (\text{SM19})$$

Here  $S(\theta, \omega, t)$  incorporates (i) the deformation of the subspace  $\text{Span}(\Psi_m, \Psi_{-m})$  into the center manifold, due to the nonlinearities; (ii) the effect of the noise, due to finite-size effects. According to the above discussion, we shall decouple these two effects, assuming that the noise is small enough so that it does not modify much the computation of the center manifold. We may assume that  $S(\theta, \omega, t)$  is “orthogonal” to the space spanned by  $\Psi_1(\theta, \omega)$  and  $\Psi_{-1}(\theta, \omega)$  (in the sense that  $(\tilde{\Psi}_{\pm 1}, S) = 0$ , where  $(,)$  denotes inner product as defined previously). Next, we use the usual center manifold ansatz [25], which assumes that  $S(\theta, \omega, t)$  may be written as a function of the amplitudes along  $\Psi_{\pm 1}(\theta, \omega)$ , i.e.,  $S(\theta, \omega, t) = W[A, A^*]$ . Hence, we may write

$$\eta(\theta, \omega, t) = A(t)\Psi_1(\theta, \omega) + A^*(t)\Psi_{-1}(\theta, \omega) + W[A, A^*]. \quad (\text{SM20})$$

The orthogonality condition gives  $(\tilde{\Psi}_{\pm 1}, W[A, A^*]) = 0$ . Taking the derivative with respect to time, we immediately get  $(\tilde{\Psi}_{\pm 1}, \partial W / \partial t) = 0$ . Now,  $\eta(\theta, \omega, t)$  is  $2\pi$ -periodic in  $\theta$ . Hence, we may expand it in a Fourier series as  $\eta(\theta, \omega, t) = \sum_{m=-\infty}^{+\infty} \eta_m(\omega, t) e^{im\theta}$ . Normalization of  $\tilde{F}_N(\theta, \omega, t)$  immediately gives  $\eta_0(\omega, t) = 0$ . Moreover, since  $\eta(\theta, \omega, t)$  is  $2\pi$ -periodic,  $W[A, A^*]$  also becomes  $2\pi$ -periodic following Eq. (SM20). Hence, we may expand it in a Fourier series as  $W[A, A^*] = \sum_{m=-\infty}^{+\infty} W_m[A, A^*] e^{im\theta}$ . Comparing the Fourier coefficients on both sides of Eq. (SM20), we obtain

$$\eta_0(\omega, t) = W_0[A, A^*] = 0, \quad (\text{SM21a})$$

$$\eta_1(\omega, t) = A(t)\psi_1(\omega) + W_1[A, A^*], \quad (\text{SM21b})$$

$$\eta_{-1}(\omega, t) = A^*(t)\psi_{-1}(\omega) + W_{-1}[A, A^*], \quad (\text{SM21c})$$

$$\eta_m(\omega, t) = W_m[A, A^*] \quad \forall |m| > 1. \quad (\text{SM21d})$$

To find the mathematical form of the above Fourier coefficients, we use the rotational symmetry of the system given by Eq. (1) of the main text. If all the oscillator phases are rotated by the same angle, i.e., under the transformation  $\theta_j \rightarrow \theta_j + \alpha \forall j$ ,  $\forall \alpha$ , Eq. (1) of the main text remains invariant. Hence, the density  $\eta(\theta, \omega, t)$  also remains invariant under this transformation. Under this transformation, clearly, the eigenfunctions of the operator  $\mathcal{L}$  transform as  $\Psi_m(\theta, \omega) \rightarrow \Psi_m(\theta, \omega) e^{im\alpha}$ . Hence, to keep  $\eta(\theta, \omega, t)$  invariant,  $A(t)$  should transform as  $A(t) \rightarrow A(t) e^{-i\alpha}$ , while  $A^*(t)$  should transform as  $A^*(t) \rightarrow A^*(t) e^{i\alpha}$ , and  $W_m[A, A^*]$  should transform as  $W_m[A, A^*] \rightarrow W_m[A, A^*] e^{-im\alpha}$ . Since,  $W_m[A, A^*]$  is a function of only  $A$  and  $A^*$ , to preserve the transformation structure, it must have the form  $W_m[A, A^*] = A^m \mathbb{W}_m(|A|^2)$ , where  $\mathbb{W}_m(|A|^2)$  may be written as  $\mathbb{W}_m(|A|^2) = w_{m,0} + w_{m,2}|A|^2 + w_{m,4}|A|^4 + \dots$ . The center manifold is tangent to the subspace  $\text{Span}(\Psi_1, \Psi_{-1})$  at  $A = A^* = 0$ ; this imposes  $W[0, 0] = \frac{\partial W}{\partial A} \Big|_{A=A^*=0} = \frac{\partial W}{\partial A^*} \Big|_{A=A^*=0} = 0$ , which gives  $w_{1,0} = 0$ . Combining all these pieces of information, we get

$$W_0[A, A^*] = 0, \quad (\text{SM22a})$$

$$W_1[A, A^*] = A|A|^2 (w_{1,2} + w_{1,4}|A|^2 + \dots), \quad (\text{SM22b})$$

$$W_m[A, A^*] = A^m (w_{m,0} + w_{m,2}|A|^2 + w_{m,4}|A|^4 + \dots) \quad \forall m > 1, \quad (\text{SM22c})$$

$$W_{-m}[A, A^*] = (W_m[A, A^*])^* \quad \forall m \neq 0. \quad (\text{SM22d})$$

Equations (SM21a) – (SM21d) and (SM22b) – (SM22d) may be written in a compact form as follows:

$$\eta_m(\omega, t) = A^m \sum_{p=0}^{+\infty} w_{m,2p} |A|^{2p}; \quad \forall m \geq 0, \quad (\text{SM23})$$

where  $w_{0,2p} = 0 \forall p$  and  $w_{1,0} = \psi_1(\omega)$  and  $w_{m,2p} = w_{m,2p}$  for any other combination of  $m > 0$  and  $p$ , and with

$$\eta_{-m}(\omega, t) = [\eta_m(\omega, t)]^*. \quad (\text{SM24})$$

We remark that from the definition of the order parameter, we have

$$\begin{aligned} Z_1 = R_1 e^{i\psi_1} &= \int_0^{2\pi} d\theta' e^{i\theta'} \int_{-\infty}^{+\infty} d\omega' \eta(\theta', \omega', t) = 2\pi \int_{-\infty}^{+\infty} d\omega' \eta_{-1}(\omega', t) \\ &= 2\pi A^* \left[ 1 + \sum_{n=1}^{+\infty} \mathcal{A}_{1,2n}^* |A|^{2n} \right] = 2\pi A^* + \mathcal{O}(A^* |A|^2), \end{aligned} \quad (\text{SM25})$$

where  $\mathcal{A}_{m,2p} \equiv \int_{-\infty}^{\infty} d\omega w_{m,2p}$ . Hence, calculating the evolution equation of the amplitude  $A(t)$  will give us the finite-size fluctuations in the order parameter  $R_1(t)$ .

We now turn to the dynamics to determine both the  $w_{m,2p}$ 's and the reduced dynamics for  $A, A^*$ . We start by taking the time derivative on the both side of Eq. (SM20), which gives

$$\frac{\partial \eta(\theta, \omega, t)}{\partial t} = \dot{A}(t) \Psi_1(\theta, \omega) + \dot{A}^*(t) \Psi_{-1}(\theta, \omega) + \frac{\partial W[A, A^*]}{\partial t}, \quad (\text{SM26})$$

where the dot represents derivative with respect to time. We now compute the inner product on both side of Eq. (SM26) with



$\tilde{\Psi}_1(\theta, \omega)$ . Using the orthonormality properties of  $\Psi_m(\theta, \omega)$  and  $\tilde{\Psi}_m(\theta, \omega)$  along with the condition on  $W [A, A^*]$ , we obtain

$$\dot{A}(t) = \left( \tilde{\Psi}_1, \frac{\partial \eta}{\partial t} \right). \quad (\text{SM27})$$

Using Eq. (SM7) in Eq. (SM27), we obtain

$$\dot{A}(t) = \left( \tilde{\Psi}_1, \mathcal{L}\eta \right) + \left( \tilde{\Psi}_1, \mathcal{N}[\eta] \right) + \left( \tilde{\Psi}_1, \sqrt{\frac{Dg(\omega)}{\pi N}} \frac{\partial \zeta(\theta, \omega, t)}{\partial \theta} \right). \quad (\text{SM28})$$

The first term on the right hand side of Eq. (SM28) gives

$$\left( \tilde{\Psi}_1, \mathcal{L}\eta \right) = \left( \mathcal{L}^\dagger \tilde{\Psi}_1, \eta \right) = \left( \lambda_{\dagger,1} \tilde{\Psi}_1, \eta \right) = \lambda_{\dagger,1}^* \left( \tilde{\Psi}_1, \eta \right) = \lambda_1 A(t). \quad (\text{SM29})$$

The second term on the right hand side of Eq. (SM28) gives

$$\left( \tilde{\Psi}_1, \mathcal{N}[\eta] \right) = \int_{-\infty}^{+\infty} d\omega' \tilde{\psi}_1^*(\omega') \mathcal{N}_1[\eta]. \quad (\text{SM30})$$

The third term on the right hand side of Eq. (SM28) gives

$$\left( \tilde{\Psi}_1, \sqrt{\frac{Dg(\omega)}{\pi N}} \frac{\partial \zeta(\theta, \omega, t)}{\partial \theta} \right) = i \sqrt{\frac{D}{\pi N}} \int_{-\infty}^{+\infty} d\omega' \tilde{\psi}_1^*(\omega') \sqrt{g(\omega')} \xi_1(\omega', t) \equiv \mathbb{O}(t). \quad (\text{SM31})$$

Clearly,  $\langle \mathbb{O}(t) \rangle = \langle \mathbb{O}(t) \mathbb{O}(t') \rangle = 0$  and  $\langle \mathbb{O}(t) \mathbb{O}^*(t') \rangle = D_{\text{eff}} (2\pi^2 N)^{-1} \delta(t - t')$ , where  $D_{\text{eff}} = D \int_{-\infty}^{+\infty} d\omega' \left| \tilde{\psi}_1(\omega') \right|^2 g(\omega')$ .

We may then replace the noise term  $\mathbb{O}(t)$  by  $\sqrt{D_{\text{eff}} (2\pi^2 N)^{-1}} \xi(t)$  with  $\langle \xi(t) \rangle = \langle \xi(t) \xi(t') \rangle = 0$  and  $\langle \xi(t) \xi^*(t') \rangle = \delta(t - t')$ . Putting all of these together along with Eqs. (SM29) and (SM30) into Eq. (SM28), we obtain

$$\dot{A}(t) = \lambda_1 A(t) + \int_{-\infty}^{+\infty} d\omega' \tilde{\psi}_1^*(\omega') \mathcal{N}_1[\eta] + \sqrt{\frac{D_{\text{eff}}}{2\pi^2 N}} \xi(t). \quad (\text{SM32})$$

We now focus on the second term on the right hand side of Eq. (SM32). Using the expression of  $\mathcal{N}_1[\eta]$  from Eq. (SM9) along with Eqs. (SM21) and (SM22), we may expand  $\mathcal{N}_1[\eta]$  in terms of  $A$  and  $A^*$ ; It reads as

$$\begin{aligned} \mathcal{N}_1[\eta] = & -A |A|^2 \pi \left[ K_1 w_{2,0} - K_2 \psi_{-1} \int_{-\infty}^{+\infty} d\omega' w_{2,0} \right] \\ & -A |A|^4 \pi \left[ K_1 \left( w_{2,2} + w_{2,0} \int_{-\infty}^{+\infty} d\omega' w_{1,2}^* \right) - K_2 \left( \psi_{-1} \int_{-\infty}^{+\infty} d\omega' w_{2,2} + w_{1,2}^* \int_{-\infty}^{+\infty} d\omega' w_{2,0} - w_{3,0} \int_{-\infty}^{+\infty} d\omega' w_{2,0}^* \right) \right. \\ & \quad \left. - K_3 w_{2,0}^* \int_{-\infty}^{+\infty} d\omega' w_{3,0} \right] \\ & -A |A|^6 \pi \left[ q K_1 \left( w_{2,4} + w_{2,2} \int_{-\infty}^{+\infty} d\omega' w_{1,2}^* + w_{2,0} \int_{-\infty}^{+\infty} d\omega' w_{1,4}^* \right) \right. \\ & \quad - K_2 \left( \psi_{-1} \int_{-\infty}^{+\infty} d\omega' w_{2,4} + w_{1,2}^* \int_{-\infty}^{+\infty} d\omega' w_{2,2} + w_{1,4}^* \int_{-\infty}^{+\infty} d\omega' w_{2,0} - w_{3,0} \int_{-\infty}^{+\infty} d\omega' w_{2,2}^* - w_{3,2} \int_{-\infty}^{+\infty} d\omega' w_{2,0}^* \right) \\ & \quad - K_3 \left( w_{2,2}^* \int_{-\infty}^{+\infty} d\omega' w_{3,0} + w_{2,0}^* \int_{-\infty}^{+\infty} d\omega' w_{3,2} - w_{4,0} \int_{-\infty}^{+\infty} d\omega' w_{3,0}^* \right) \\ & \quad \left. - K_4 w_{3,0}^* \int_{-\infty}^{+\infty} d\omega' w_{4,0} \right] + \dots, \end{aligned} \quad (\text{SM33})$$

where  $w_{1,2}, w_{2,0}, w_{2,2}, w_{3,0}$  and  $\psi_{-1}$  are functions of  $\omega$ . Interestingly, the coefficient of  $A|A|^{2b}$  only depends on  $K_1, \dots, K_{b+1}$ .

Using Eq. (SM32), we obtain

$$\int_{-\infty}^{+\infty} d\omega' \tilde{\psi}_1^*(\omega') \mathcal{N}_1[\eta] = -c_3 A|A|^2 - c_5 A|A|^4 + \dots, \quad (\text{SM34})$$

where we have

$$c_3 \equiv \pi \left[ K_1 \int_{-\infty}^{+\infty} d\omega' \tilde{\psi}_1^* w_{2,0} - K_2 \int_{-\infty}^{+\infty} d\omega' \tilde{\psi}_1^* \psi_{-1} \int_{-\infty}^{+\infty} d\omega' w_{2,0} \right], \quad (\text{SM35})$$

$$c_5 \equiv \pi \left[ K_1 \left( \int_{-\infty}^{+\infty} d\omega' \tilde{\psi}_1^* w_{2,2} + \int_{-\infty}^{+\infty} d\omega' \tilde{\psi}_1^* w_{2,0} \int_{-\infty}^{+\infty} d\omega' w_{1,2}^* \right) - K_2 \left( \int_{-\infty}^{+\infty} d\omega' \tilde{\psi}_1^* \psi_{-1} \int_{-\infty}^{+\infty} d\omega' w_{2,2} \right. \right. \\ \left. \left. + \int_{-\infty}^{+\infty} d\omega' \tilde{\psi}_1^* w_{1,2}^* \int_{-\infty}^{+\infty} d\omega' w_{2,0} - \int_{-\infty}^{+\infty} d\omega' \tilde{\psi}_1^* w_{3,0} \int_{-\infty}^{+\infty} d\omega' w_{2,0}^* \right) - K_3 \int_{-\infty}^{+\infty} d\omega' \tilde{\psi}_1^* w_{2,0}^* \int_{-\infty}^{+\infty} d\omega' w_{3,0} \right] \quad (\text{SM36})$$

Now, we have to find the expression of  $w_{m,2p}$ 's. Here, we sketch the method for finding  $w_{2,0}$ . The rest of the computation for other  $w_{m,2p}$ 's may be pursued in a similar way. We start from Eq. (SM26). Combining it with Eqs. (SM7) and (SM20), we obtain

$$\frac{\partial W}{\partial t} = \mathcal{L}W + \mathcal{N}[\eta] + i\sqrt{\frac{Dg(\omega)}{\pi N}} \sum_{m=-\infty}^{+\infty} m \xi_m(\omega, t) e^{im\theta} - \left[ (\dot{A} - \lambda_1 A) \Psi_1(\theta, \omega) + \text{c.c.} \right], \quad (\text{SM37})$$

where c.c. means complex conjugate. Comparing the second Fourier mode of both sides of Eq. (SM37), we obtain

$$\frac{dW_2}{dt} = L_2 W_2 + \mathcal{N}_2[\eta] + i\sqrt{\frac{4Dg(\omega)}{\pi N}} \xi_2(\omega, t). \quad (\text{SM38})$$

The left hand side of Eq. (SM38) to leading order gives:  $dW_2/dt \approx 2A\dot{A}w_{2,0} \approx 2\lambda_1 A^2 w_{2,0}$ . Using Eq. (SM8), the first term on the right hand side of Eq. (SM38) to leading order gives  $L_2 W_2 \approx -(4D + i2\omega)A^2 w_{2,0} + K_2 g(\omega)A^2 \int_{-\infty}^{\infty} d\omega' w_{2,0}$ . Similarly, using Eq. (SM9), the second term on the right hand side of Eq. (SM38) to leading order gives  $\mathcal{N}_2[\eta] \approx 2\pi K_1 A^2 \psi_1(\omega)$ . Furthermore, if  $N$  is large enough, we may ignore the third term on the right hand side of Eq. (SM38). Combining all of these, we finally obtain

$$w_{2,0} = \frac{\pi K_1 \psi_1(\omega)}{(\lambda_1 + 2D + i\omega)} + \frac{K_2 g(\omega)}{2(\lambda_1 + 2D + i\omega)} \int_{-\infty}^{\infty} d\omega' w_{2,0}. \quad (\text{SM39})$$

Following similar steps, we find the rest of the  $w_{a,b}$ 's, which read as

$$w_{3,0} = \frac{\pi [K_1 w_{2,0} + K_2 \psi_1(\omega) \int_{-\infty}^{\infty} d\omega' w_{2,0}]}{(\lambda_1 + 3D + i\omega)} + \frac{K_3 g(\omega)}{2(\lambda_1 + 3D + i\omega)} \int_{-\infty}^{\infty} d\omega' w_{3,0}, \quad (\text{SM40})$$

and

$$w_{1,2} = \frac{c_3 \psi_1(\omega) - \pi [K_1 w_{2,0} - K_2 \psi_{-1}(\omega) \int_{-\infty}^{\infty} d\omega' w_{2,0}]}{(2\lambda_1 + \lambda_1^* + D + i\omega)} + \frac{K_1 g(\omega)}{2(2\lambda_1 + \lambda_1^* + D + i\omega)} \int_{-\infty}^{\infty} d\omega' w_{1,2}, \quad (\text{SM41})$$

$$w_{2,2} = \frac{2c_3 w_{2,0} + 2\pi K_1 [w_{1,2} + \psi_1(\omega) \int_{-\infty}^{+\infty} d\omega' w_{1,2} - w_{3,0}] + 2\pi K_3 \psi_{-1}(\omega) \int_{-\infty}^{+\infty} d\omega' w_{3,0}}{(3\lambda_1 + \lambda_1^* + 4D + i2\omega)} \\ + \frac{K_2 g(\omega)}{(3\lambda_1 + \lambda_1^* + 4D + i2\omega)} \int_{-\infty}^{\infty} d\omega' w_{2,2}. \quad (\text{SM42})$$

We observe that all the  $w_{m,2p}$ 's computed till now have the following self-consistent form

$$w_{m,2p} = a^{(m,2p)}(w) + b^{(m,2p)}(w) \int_{-\infty}^{\infty} d\omega' w_{m,2p}. \quad (\text{SM43})$$

From these equations, to obtain an expression of  $w_{m,2p}$ , we first integrate Eq. (SM43) with respect to  $\omega$  and rearrange it to obtain

an expression of  $\int_{-\infty}^{\infty} d\omega' w_{m,2p}$ . Putting it back into Eq. (SM43), we finally obtain

$$w_{m,2p} = a^{(m,2p)}(w) + b^{(m,2p)}(\omega) \frac{\int_{-\infty}^{\infty} d\omega' a^{(m,2p)}(w')}{1 - \int_{-\infty}^{\infty} d\omega' b^{(m,2p)}(w')}. \quad (\text{SM44})$$

We have now calculated all relevant quantities. Combining everything we have, we may express Eq. (SM32) as

$$\dot{A}(t) = \lambda_1 A(t) - c_3 A|A|^2 - c_5 A|A|^4 + \sqrt{\frac{D_{\text{eff}}}{2\pi^2 N}} \xi(t). \quad (\text{SM45})$$

Proceeding as above, we obtain in general that

$$\dot{A}(t) = \lambda_1 A(t) - \sum_{n=1}^{\infty} c_{2n+1} A|A|^{2n} + \sqrt{\frac{D_{\text{eff}}}{2\pi^2 N}} \xi(t), \quad (\text{SM46})$$

where we have

$$c_{2n+1} = \pi \sum_{l=1}^{\infty} K_l \sum_{q=0}^{n-l+1} \left[ \mathcal{B}_{l+1,2q} \mathcal{A}_{l,2(n-l-q)}^* \Theta(n-l-q) - \mathcal{C}_{l-1,2q}^* \mathcal{A}_{l,2(n-l+1-q)} \right], \quad (\text{SM47})$$

for  $n = 1, 2, \dots$  and  $\Theta(x) = 1 \forall x \geq 0$  and  $\Theta(x) = 0 \forall x < 0$ , and with

$$\mathcal{A}_{m,2p} \equiv \int_{-\infty}^{\infty} d\omega w_{m,2p}, \quad (\text{SM48})$$

$$\mathcal{B}_{m,2p} \equiv \int_{-\infty}^{\infty} d\omega \tilde{\psi}_1^* w_{m,2p}, \quad (\text{SM49})$$

$$\mathcal{C}_{m,2p} \equiv \int_{-\infty}^{\infty} d\omega \tilde{\psi}_1 w_{m,2p}, \quad (\text{SM50})$$

where we have

$$\begin{aligned} w_{m,2p} = & \left[ \frac{1}{(m+p)\lambda_1 + p\lambda_1^* + m^2 D + im\omega} \right] \left[ \sum_{q=0}^{p-1} \left[ (m+q)c_{2(p-q)+1} + q\mathcal{C}_{2(p-q)+1}^* \right] w_{m,2q} \right. \\ & + m\pi \sum_{l=1}^m K_l \sum_{q=0}^p w_{m-l,2q} \mathcal{A}_{l,2(p-q)} + m\pi \sum_{l=m+1}^{\infty} K_l \sum_{q=0}^{m+p-l} w_{l-m,2q}^* \mathcal{A}_{l,2(m+p-l-q)} \\ & \left. - m\pi \sum_{l=1}^{\infty} K_l \sum_{q=0}^{p-l} w_{m+l,2q} \mathcal{A}_{l,2(p-l-q)} + \frac{mK_m}{2} g(\omega) \mathcal{A}_{m,2p} \right], \quad (\text{SM51}) \end{aligned}$$

and  $w_{0,2p} = 0 \forall p$  and  $w_{1,0} = \psi_1(\omega)$ . With these notations, Eqs. (SM35) and (SM36) become

$$c_3 = \pi \left[ K_1 \mathcal{B}_{2,0} - K_2 \mathcal{C}_{1,0}^* \mathcal{A}_{2,0} \right], \quad (\text{SM52})$$

$$c_5 = \pi \left[ K_1 \left( \mathcal{B}_{2,2} + \mathcal{A}_{1,2}^* \mathcal{B}_{2,0} \right) - K_2 \left( \mathcal{C}_{1,0}^* \mathcal{A}_{2,2} + \mathcal{C}_{1,2}^* \mathcal{A}_{2,0} - \mathcal{A}_{2,0}^* \mathcal{B}_{3,0} \right) - K_3 \mathcal{C}_{2,0}^* \mathcal{A}_{3,0} \right]. \quad (\text{SM53})$$

Equation (SM46) is Eq. (5) of the main text.

### Appendix B: Derivation of Eq. (6) of the main text

Let us start from the reduced equation (SM46) and define  $A \equiv r e^{i\psi} = x + iy$ . Hence, we have  $r = |A|$ . We now compute the steady-state distribution of  $r$ . Decomposing Eq. (SM46) into its real and imaginary components, we obtain

$$\frac{dx}{dt} = \lambda_1 x - \sum_{n=1}^{\infty} c_{2n+1} x (x^2 + y^2)^n + \sqrt{\frac{D_{\text{eff}}}{4\pi^2 N}} \xi_R(t), \quad (\text{SM1})$$

$$\frac{dy}{dt} = \lambda_1 y - \sum_{n=1}^{\infty} c_{2n+1} y (x^2 + y^2)^n + \sqrt{\frac{D_{\text{eff}}}{4\pi^2 N}} \xi_I(t), \quad (\text{SM2})$$

with  $\xi(t) = \frac{1}{\sqrt{2}} \xi_R(t) + i \frac{1}{\sqrt{2}} \xi_I(t)$  with  $\langle \xi_R(t) \xi_R(t') \rangle = \langle \xi_I(t) \xi_I(t') \rangle = \delta(t - t')$  and  $\langle \xi_R(t) \rangle = \langle \xi_I(t) \rangle = \langle \xi_I(t) \xi_R(t') \rangle = 0$ . The drift term in Eqs. (SM1) and (SM2) are negative of the gradient of the function

$$V(x, y) = \sum_{n \geq 0} \frac{c_{2n+1}}{2(n+1)} (x^2 + y^2)^{n+1}, \quad (\text{SM3})$$

where we have defined  $c_1 \equiv -\lambda_1$  to shorten the equations. Hence, the steady state probability distribution for (SM1)- (SM2) is

$$P(x, y) = \mathcal{N} \exp \left( N \frac{8\pi^2}{D_{\text{eff}}} V(x, y) \right), \quad (\text{SM4})$$

where  $\mathcal{N}$  is a normalization. Performing the polar change of variable from  $(x, y)$  to  $(r, \theta)$ , and noting that  $P$  is rotationally symmetric, we obtain the steady state distribution for  $r$

$$\mathbf{P}(r) = \mathcal{M} r \exp \left\{ - \frac{8\pi^2 N}{D_{\text{eff}}} \sum_{n=0}^{\infty} \frac{c_{2n+1} r^{2(n+1)}}{2(n+1)} \right\}, \quad (\text{SM5})$$

where  $\mathcal{M}$  is a normalization constant. The above is Eq. (6) of the main text.

### Appendix C: Results corresponding to the model in Application 1 of the main text

In Application 1: Stochastic Kuramoto model with harmonic and bi-harmonic interaction and without frequency, we consider

$$K_m = 0 \quad \forall m \geq 3, \quad \text{and} \quad g(\omega) = \delta(\omega). \quad (\text{SM1})$$

In this case, we could remove altogether the variable  $\omega$ , working with functions of  $\theta$  only. However, in order to fit all applications in the same framework and apply the general formulas, we shall keep the variable  $\omega$ ; in any case, the computations simplify a lot. Following Eq. (SM12), the spectral function becomes

$$\Lambda_m(x) = 1 - \frac{|m| K_{|m|}}{2(x + m^2 D)}, \quad \text{with } |m| = 1, 2. \quad (\text{SM2})$$

The roots of this spectral function give the eigenvalues, which read as

$$\lambda_{\pm 1} = \frac{K_1}{2} - D, \quad \lambda_{\pm 2} = K_2 - 4D. \quad (\text{SM3})$$

For  $|m| > 2$  we obtain  $\lambda_m = -m^2 D$ . The eigenfunctions are the complex exponentials:  $\Psi_m = \psi_1(\omega) e^{im\theta} = \delta(\omega) e^{im\theta}$ ,  $m \in \mathbb{Z}$ .

We are interested in the transition of  $R_1$ . Hence, the relevant eigenfunction is  $\Psi_{\pm 1}$ . Corresponding adjoint eigenfunctions, properly normalized, are:

$$\tilde{\Psi}_{\pm 1} = \frac{1}{2\pi} \tilde{\psi}_{\pm 1}(\omega) e^{\pm i\theta} = \frac{1}{2\pi} \left( \frac{K_1}{K_1 \mp i2\omega} \right) e^{\pm i\theta}. \quad (\text{SM4})$$

Since  $\tilde{\Psi}_{\pm 1}$  will always appear in conjunction with a  $\delta(\omega)$  factor, its apparent dependency on the variable  $\omega$  will have no influence

on the following computations. Evaluating the relevant expressions in Eq. (SM52), we obtain

$$\mathcal{C}_{1,0} = 1, \mathcal{A}_{2,0} = \mathcal{B}_{2,0} = \frac{2\pi K_1}{K_1 - K_2 + 2D}. \quad (\text{SM5})$$

Using these expressions, we obtain  $c_3$  from Eq. (SM52) as

$$c_3 = 2\pi^2 K_1 \left( \frac{K_1 - K_2}{K_1 - K_2 + 2D} \right). \quad (\text{SM6})$$

Using the expression of  $c_3$ , we further obtain

$$\begin{aligned} \mathcal{A}_{1,2} &= 0, \quad \mathcal{A}_{2,2} = \mathcal{B}_{2,2} = \frac{8\pi^3 K_1^2 [K_2^2 - K_2(K_1 + 6D) + 2DK_1]}{(K_1 + 4D)(K_1 - K_2 + 2D)^2(2K_1 - K_2)}, \\ \mathcal{C}_{1,2} &= 0, \quad \mathcal{B}_{3,0} = \frac{4\pi^2 K_1 (K_1 + K_2)}{(K_1 + 4D)(K_1 - K_2 + 2D)}. \end{aligned} \quad (\text{SM7})$$

Using all of these in Eq. (SM53), we obtain

$$c_5 = \frac{8\pi^4 K_1^2 [2D(K_1 - 3K_2)(K_1 - K_2) + K_2(K_1^2 + 3K_1 K_2 - 2K_2^2)]}{(K_1 + 4D)(K_1 - K_2 + 2D)^2(2K_1 - K_2)}. \quad (\text{SM8})$$

From the definition of  $D_{\text{eff}}$ , we further get

$$D_{\text{eff}} = D \int_{-\infty}^{+\infty} d\omega' \left| \tilde{\psi}_1(\omega') \right|^2 g(\omega') = D \int_{-\infty}^{+\infty} d\omega' \left| \frac{K_1}{K_1 \mp i2\omega'} \right|^2 \delta(\omega') = D. \quad (\text{SM9})$$

For this particular model, we may simplify the recursion relation, Eq. (SM51). Since we have  $K_{|m|} = 0 \forall |m| > 2$ , we may simplify Eq. (SM51) for  $m = 1$  as

$$\begin{aligned} w_{1,2p} &= \left[ \frac{1}{(1+2p)\lambda_1 + D + i\omega} \right] \left[ \sum_{q=0}^{p-1} \left[ (1+q)c_{2(p-q)+1} + qc_{2(p-q)+1}^* \right] w_{1,2q} \right. \\ &\quad \left. + \pi K_2 \sum_{q=0}^{p-1} w_{1,2q}^* \mathcal{A}_{2,2(m+p-l-q)} - \pi \sum_{l=1}^2 K_l \sum_{q=0}^{p-l} w_{1+l,2q} \mathcal{A}_{l,2(p-l-q)} + \frac{K_1}{2} g(\omega) \mathcal{A}_{1,2p} \right], \end{aligned}$$

and for  $m > 2$  as

$$\begin{aligned} w_{m,2p} &= \left[ \frac{1}{(m+2p)\lambda_1 + m^2 D + im\omega} \right] \left[ \sum_{q=0}^{p-1} \left[ (m+q)c_{2(p-q)+1} + qc_{2(p-q)+1}^* \right] w_{m,2q} \right. \\ &\quad \left. + m\pi \sum_{l=1}^2 K_l \sum_{q=0}^p w_{m-l,2q} \mathcal{A}_{l,2(p-q)} - m\pi \sum_{l=1}^2 K_l \sum_{q=0}^{p-l} w_{m+l,2q} \mathcal{A}_{l,2(p-l-q)} + \frac{mK_m}{2} \delta(\omega) \mathcal{A}_{m,2p} \right], \end{aligned}$$

where we have used the result  $w_{0,2p} = 0 \forall p$  and  $\lambda_1 = \lambda_1^*$  for this model. Now we have  $w_{0,2p} = 0 \forall p$  and  $w_{1,0} = \psi_1(\omega) = \delta(\omega)$ . This immediately gives  $\mathcal{A}_{1,0} = \mathcal{B}_{1,0} = \mathcal{C}_{1,0} = 1$ . We now focus on obtaining  $w_{m,0}$ . Putting  $p = 0$  in Eq. (SM10), we obtain for  $m \geq 2$  that

$$w_{m,0} = \left[ \frac{1}{m\lambda_1 + m^2 D + im\omega} \right] \left[ m\pi K_1 w_{m-1,0} \mathcal{A}_{1,0} + m\pi K_2 w_{m-2,0} \mathcal{A}_{2,0} + \frac{mK_m}{2} \delta(\omega) \mathcal{A}_{m,0} \right]. \quad (\text{SM10})$$

Hence, for  $m = 2$ , we have

$$w_{2,0} = \left[ \frac{1}{2\lambda_1 + 4D + i2\omega} \right] [2\pi K_1 w_{1,0} \mathcal{A}_{1,0} + K_2 \delta(\omega) \mathcal{A}_{2,0}] = \left[ \frac{2\pi K_1 \mathcal{A}_{1,0} + K_2 \mathcal{A}_{2,0}}{2\lambda_1 + 4D} \right] \delta(\omega). \quad (\text{SM11})$$



Integrating both sides with respect to  $\omega$  and noting that  $\mathcal{A}_{2,0} = \int_{-\infty}^{\infty} d\omega w_{2,0}$ , we obtain

$$w_{2,0} = \mathcal{A}_{2,0} \delta(\omega) = \left[ \frac{2\pi K_1}{K_1 - K_2 + 2D} \right] \delta(\omega). \quad (\text{SM12})$$

Since  $w_{1,0}$  and  $w_{2,0}$  are proportional to  $\delta(\omega)$ , then using Eq. (SM10) we deduce that any  $w_{m,0}$  is proportional to  $\delta(\omega)$ . Hence, we may write  $w_{m,0} = \mathcal{A}_{m,0} \delta(\omega)$  and use this in Eq. (SM10) to obtain

$$w_{m,0} = \pi \left[ \frac{K_1 \mathcal{A}_{m-1,0} + K_2 \mathcal{A}_{m-2,0} \mathcal{A}_{2,0}}{\lambda_1 + mD} \right] \delta(\omega), \quad (\text{SM13})$$

where  $\mathcal{A}_{m,0}$ 's can be obtained from the recursion relation as

$$\mathcal{A}_{m,0} = \pi \left[ \frac{K_1 \mathcal{A}_{m-1,0} + K_2 \mathcal{A}_{m-2,0} \mathcal{A}_{2,0}}{\lambda_1 + mD} \right], \quad (\text{SM14})$$

for  $m \geq 2$ , and  $\mathcal{A}_{2,0}$  and  $\mathcal{A}_{1,0}$  are known.

Let us now focus on Eq. (SM10). We observe that any  $w_{m,2p}$  is expressible as a linear combination of those  $w_{m',2p'}$  that satisfy  $m' + 2p' \leq m + 2p$  with  $m' = m - 2, m - 1, m, m + 1$ , and  $m + 1$ . Now, if all those  $w_{m',2p'}$  have a form  $w_{m',2p'} = \mathcal{A}_{m',2p'} \delta(\omega)$ , where  $\mathcal{A}_{m',2p'} = \int_{-\infty}^{\infty} d\omega w_{m',2p'}$  is a constant, then  $w_{m,2p}$  can also be written as

$$w_{m,2p} = \mathcal{A}_{m,2p} \delta(\omega), \quad (\text{SM15})$$

with the recursion relation of  $\mathcal{A}_{m,2p}$ 's reading for  $m = 1$  as

$$\begin{aligned} \mathcal{A}_{1,2p} = & \frac{1}{2p\lambda_1} \left[ \sum_{q=0}^{p-1} (1+2q) c_{2(p-q)+1} \mathcal{A}_{1,2q} + \pi K_2 \sum_{q=0}^{p-1} \mathcal{A}_{1,2q} \mathcal{A}_{2,2(p-q-1)} - \pi K_1 \sum_{q=0}^{p-1} \mathcal{A}_{2,2q} \mathcal{A}_{1,2(p-q-1)} \right. \\ & \left. - \pi K_2 \sum_{q=0}^{p-2} \mathcal{A}_{3,2q} \mathcal{A}_{2,2(p-q-2)} \Theta(p-2) \right], \end{aligned} \quad (\text{SM16})$$

and for  $m > 2$  as

$$\begin{aligned} \mathcal{A}_{m,2p} = & \left[ \frac{1}{(m+2p)\lambda_1 + m^2 D} \right] \left[ \sum_{q=0}^{p-1} [(m+2q) c_{2(p-q)+1}] \mathcal{A}_{m,2q} \right. \\ & \left. + m\pi \sum_{l=1}^2 K_l \sum_{q=0}^p \mathcal{A}_{m-l,2q} \mathcal{A}_{l,2(p-q)} - m\pi \sum_{l=1}^2 K_l \sum_{q=0}^{p-l} \mathcal{A}_{m+l,2q} \mathcal{A}_{l,2(p-l-q)} + \frac{mK_m}{2} \mathcal{A}_{m,2p} \right]. \end{aligned} \quad (\text{SM17})$$

From Eq. (SM15), we immediately have  $\mathcal{A}_{m,2p} = \mathcal{B}_{m,2p} = \mathcal{C}_{m,2p} \in \mathbb{R} \forall m, p$  for this model. Hence, we can simplify Eq. (SM47) for this model as

$$c_{2n+1} = \pi K_1 \sum_{q=0}^{n-1} \mathcal{A}_{2,2q} \mathcal{A}_{1,2(n-q-1)} + \pi K_2 \sum_{q=0}^{n-2} \mathcal{A}_{3,2q} \mathcal{A}_{2,2(n-q-2)} \Theta(n-q-2) - \pi K_2 \sum_{q=0}^{n-1} \mathcal{A}_{1,2q} \mathcal{A}_{2,2(n-q-1)}. \quad (\text{SM18})$$

Let us now focus on  $\mathcal{A}_{1,2p}$ 's. We already have  $\mathcal{A}_{1,0} = 1$ . Now, from Eq. (SM16), we obtain

$$\mathcal{A}_{1,2} = \frac{1}{2p\lambda_1} [c_3 + \pi K_2 \mathcal{A}_{1,0} \mathcal{A}_{2,0} - \pi K_1 \mathcal{A}_{2,0}] = 0, \quad (\text{SM19})$$

since by definition  $c_3 = \pi [K_1 \mathcal{B}_{2,0} - K_2 \mathcal{C}_{1,0}^* \mathcal{A}_{2,0}] = \pi [K_1 \mathcal{A}_{2,0} - K_2 \mathcal{A}_{1,0} \mathcal{A}_{2,0}]$ . Let us now prove by induction that  $\mathcal{A}_{1,2p} = 0 \forall p > 0$ . We have already proved that  $\mathcal{A}_{1,2} = 0$ . Now, let us assume that  $\mathcal{A}_{1,4} = \mathcal{A}_{1,6} = \dots = \mathcal{A}_{1,2(p-1)} = 0$ . Putting this

condition in Eq. (SM16), we obtain

$$\mathcal{A}_{1,2p} = \frac{1}{2p\lambda_1} \left[ c_{2p+1} - \pi K_1 \mathcal{A}_{2,2(p-1)} - \pi K_2 \sum_{q=0}^{p-2} \mathcal{A}_{3,2q} \mathcal{A}_{2,2(p-q-2)} \right] = 0. \quad (\text{SM20})$$

In the last step, we have used the expression of  $c_{2p+1}$  from Eq. (SM18) with the condition  $\mathcal{A}_{1,2m} = 0 \forall m \in \{1, 2, \dots, p-1\}$ . Hence, by the method of induction, we have proved  $\mathcal{A}_{1,2p} = 0 \forall p \geq 1$ .

Using these results, we may simplify Eqs. (SM47) and (SM51) as

$$c_{2n+1} = \pi \left[ (K_1 - K_2) \mathcal{A}_{2,2(n-1)} + K_2 \sum_{j=0}^{n-2} \mathcal{A}_{2,2j} \mathcal{A}_{3,2(n-j-2)} \right], \quad (\text{SM21})$$

where

$$w_{m,2l} = \frac{1}{[(m+2l)\lambda_1 + m^2 D]} \left[ \sum_{j=0}^{l-1} (m+2j) c_{2(l-j)+1} \mathcal{A}_{m,2j} + m\pi K_1 (\mathcal{A}_{m-1,2l} - \mathcal{A}_{m+1,2(l-1)}) \right. \\ \left. + m\pi K_2 \sum_{j=0}^l \mathcal{A}_{2,2j} (\mathcal{A}_{m-2,2(l-j)} - \mathcal{A}_{m+2,2(n-j-2)} \Theta(n-j-2)) \right], \quad (\text{SM22})$$

for  $n = 1, 2, 3, \dots$  and with  $w_{0,2l} = 0 \forall l$  and  $w_{1,0} = 1$  and  $w_{1,2l} = 0 \forall l > 0$  and  $\Theta(x) = 1 \forall x \geq 0$  and  $\Theta(x) = 0 \forall x < 0$ . Using these relations recursively, we may calculate  $c_{2n+1}$  for any  $n$ .

#### Appendix D: Results corresponding to the model in Application 2 of the main text

In Application 2: Stochastic Kuramoto model with harmonic and bi-harmonic interaction with bi-delta frequency, we consider

$$K_m = 0 \forall m \geq 3, \text{ and } g(\omega) = \frac{1}{2} \delta(\omega - \omega_0) + \frac{1}{2} \delta(\omega + \omega_0). \quad (\text{SM1})$$

As discussed in the main text, when  $N$  is finite, the density  $\bar{g}_N(\omega) = \sum_{j=1}^N \delta(\omega - \omega_j)$  will not exactly match with  $g(\omega)$ . However, we may in any case write  $\bar{g}_N(\omega) = \alpha \delta(\omega - \omega_0) + (1 - \alpha) \delta(\omega + \omega_0)$ , incorporating in this case the finite-size effects from frequency disorder. For this specific frequency distribution, we could simplify the dependency on the  $\omega$  variable by using two-components distribution functions, for  $\pm \omega_0$ . However, as for application 1, in order to apply the general formulas, we shall keep the variable  $\omega$  as if it were continuous. In a typical frequency realization, the finite-size parameter  $\alpha$  is such that  $\alpha \rightarrow 1/2$  as  $N \rightarrow \infty$ . Following Eq. (SM12), the spectral function becomes

$$\Lambda_m(x) = 1 - \frac{|m|K_{|m|} [x + m^2 D + i(1 - 2\alpha)m\omega_0]}{2 [(x + m^2 D)^2 + m^2 \omega_0^2]}, \text{ with } |m| = 1, 2. \quad (\text{SM2})$$

The roots of this spectral function give the eigenvalues, which read as

$$\lambda_{m,\pm} = -m^2 D + \frac{|m|K_m}{2} \left[ \frac{1}{2} \pm \sqrt{\left( \frac{1}{4} - \frac{4\omega_0^2}{K_m^2} \right) + i2(1 - 2\alpha) \frac{|m|\omega_0}{mK_m}} \right], \text{ with } |m| = 1, 2. \quad (\text{SM3})$$

The eigenfunctions corresponding to these eigenvalues are given by Eq. (SM13). Putting  $\omega_0 = 0$ , we get back the eigenvalues given in Eq. (SM3). For  $|m| \geq 3$ , the eigenvalues are  $\lambda_{m,\pm} = -m^2 D \pm im\omega_0$  with the corresponding eigenfunction  $\psi_{m,\pm}(\omega) = \delta(\omega \pm \omega_0)$ . The spectral analysis for  $|m| \geq 3$  will not be needed. Note that, unlike the previous example, here for each Fourier mode  $m = \pm 1, \pm 2$ , there are two eigenvalues and two corresponding eigenfunctions, denoted by  $\pm$ . In this case the two eigenfunction of  $\mathcal{L}$  corresponding to the  $m$ th mode may be written as, following Eq. (SM13)

$$\psi_{m,\pm}(\omega) = \frac{|m|K_{|m|}}{4(\lambda_{m,\pm} + m^2 D + im\omega_0)} \delta(\omega - \omega_0) + \frac{|m|K_{|m|}}{4(\lambda_{m,\pm} + m^2 D - im\omega_0)} \delta(\omega + \omega_0). \quad (\text{SM4})$$

Clearly, the two eigenfunctions  $\psi_{m,\pm}(\omega)$  lie on the two-dimensional space spanned by  $\delta(\omega - \omega_0)$  and  $\delta(\omega + \omega_0)$ . Following Eq. (SM18), we have the eigenfunctions of  $\mathcal{L}^\dagger$  which read

$$\tilde{\psi}_{1,\pm}(\omega) = \frac{\mathcal{G}_\pm^*}{(\lambda_{1,\pm}^* + D - i\omega)}, \quad \mathcal{G}_\pm = \frac{2 \left[ (\lambda_{1,\pm} + D)^2 + \omega_0^2 \right]^2}{K_1 \left[ (\lambda_{1,\pm} + D)^2 - \omega_0^2 + i2(1 - 2\alpha)\omega_0 (\lambda_{1,\pm} + D) \right]}. \quad (\text{SM5})$$

As discussed in the main text, in the region of our interest, the relevant unstable mode is  $\psi_{1,+}$ . In this case, evaluating the relevant expressions in Eq. (SM52), we obtain

$$\mathcal{C}_{1,0}^* = \frac{K_1}{2} \mathcal{G}_+ \mathcal{H}, \quad \text{where } \mathcal{H} \equiv \frac{(\lambda_{1,+} + D)(\lambda_{1,+}^* + D) + \omega_0^2 + i(1 - 2\alpha)\omega_0(\lambda_{1,+}^* - \lambda_{1,+})}{\left[ (\lambda_{1,+} + D)^2 + \omega_0^2 \right]^2}, \quad (\text{SM6})$$

$$\mathcal{A}_{2,0} = \frac{\pi K_1^2 \left[ (\lambda_{1,+} + 2D)(\lambda_{1,+} + D) - \omega_0^2 + i(1 - 2\alpha)\omega_0(2\lambda_{1,+} + 3D) \right]}{2 \left[ (\lambda_{1,+} + D)^2 + \omega_0^2 \right] \left[ (\lambda_{1,+} + 2D)^2 + \omega_0^2 - \left( \frac{K_2}{2} \right) (\lambda_{1,+} + 2D + i(1 - 2\alpha)\omega_0) \right]}, \quad (\text{SM7})$$

$$\mathcal{B}_{2,0} = \frac{\pi K_1^2}{2} \mathcal{G}_+ \mathcal{J} + \frac{K_2}{2} \mathcal{G}_+ \mathcal{A}_{2,0} \mathcal{K} \quad \text{where, } \mathcal{K} \equiv \frac{(\lambda_{1,+} + 2D)(\lambda_{1,+} + D) - \omega_0^2 + i(1 - 2\alpha)\omega_0(2\lambda_{1,+} + 3D)}{\left[ (\lambda_{1,+} + 2D)^2 + \omega_0^2 \right] \left[ (\lambda_{1,+} + D)^2 + \omega_0^2 \right]} \quad (\text{SM8})$$

and

$$\mathcal{J} \equiv \frac{\left[ (\lambda_{1,+} + D)^2 (\lambda_{1,+} + 2D) - \omega_0^2 (3\lambda_{1,+} + 4D) \right] + i(1 - 2\alpha)\omega_0 \left[ (\lambda_{1,+} + D)^2 - \omega_0^2 + 2(\lambda_{1,+} + D)(\lambda_{1,+} + 2D) \right]}{\left[ (\lambda_{1,+} + D)^2 + \omega_0^2 \right]^2 \left[ (\lambda_{1,+} + 2D)^2 + \omega_0^2 \right]} \quad (\text{SM9})$$

Using these expressions, we obtain  $c_3$  from Eq. (SM52), which reads as

$$c_3 = \frac{\pi K_1}{2} \mathcal{G}_+ \left[ \pi K_1^2 \mathcal{J} + K_2 \mathcal{A}_{2,0} (\mathcal{K} - \mathcal{H}) \right]. \quad (\text{SM10})$$

Putting  $\omega_0 = 0$  in Eq. (SM10), we get back Eq. (SM6). To write the expression of  $c_5$ , let us define a functional  $\mathbb{P}[x(\cdot)] = \frac{\alpha}{x(\omega_0)} + \frac{1-\alpha}{x(-\omega_0)}$ , to make the expressions look neat. Here, given that  $x(\omega_0)$  is a function of  $\omega_0$ , the quantity  $x(-\omega_0)$  is what we obtain replacing  $\omega_0$  by  $-\omega_0$  in the expression of  $x(\omega_0)$ . In this way, we may write

$$\mathcal{A}_{1,2} = \frac{\mathcal{D}_1}{1 - \mathcal{D}_0}, \quad \text{where } \mathcal{D}_0 = \frac{K_1}{2} \mathbb{P}[x_5], \quad \mathcal{D}_1 = \frac{K_1}{2} c_3 \mathbb{P}[x_1 x_5] - \frac{\pi^2 K_1^3}{2} \mathbb{P}[x_1 x_2 x_5] - \frac{\pi K_1 K_2}{2} \mathcal{B} \{ \mathbb{P}[x_2 x_5] - \mathbb{P}[x_{-1} x_5] \}, \quad (\text{SM11})$$

$$\mathcal{A}_{2,2} = \frac{\mathcal{E}_1}{1 - \mathcal{E}_0}, \quad \text{where } \mathcal{E}_0 = K_2 \mathbb{P}[x_4], \quad (\text{SM12})$$

$$\mathcal{E}_1 = \pi K_1^2 \mathcal{A}_{1,2} \{ \mathbb{P}[x_1 x_4] + \mathbb{P}[x_4 x_5] \} + \pi K_1^2 c_3 \{ \mathbb{P}[x_1 x_2 x_4] + \mathbb{P}[x_1 x_4 x_5] \} - \pi^3 K_1^4 \{ \mathbb{P}[x_1 x_2 x_3 x_4] + \mathbb{P}[x_1 x_2 x_4 x_5] \} + K_2 c_3 \mathcal{A}_{2,0} \mathbb{P}[x_2 x_4] - \pi^2 K_1^2 K_2 \mathcal{A}_{2,0} \{ \mathbb{P}[x_1 x_3 x_4] + \mathbb{P}[x_2 x_3 x_4] + \mathbb{P}[x_2 x_4 x_5] - \mathbb{P}[x_1^* x_4 x_5] \}, \quad (\text{SM13})$$

where  $x_1(\omega_0) = (\lambda_{1,+} + D + i\omega_0)$ ,  $x_{-1}(\omega_0) = (\lambda_{1,+} + D - i\omega_0)$ ,  $x_2(\omega_0) = (\lambda_{1,+} + 2D + i\omega_0)$ ,  $x_3(\omega_0) = (\lambda_{1,+} + 3D + i\omega_0)$ , and moreover that  $x_4(\omega_0) = (3\lambda_{1,+} + \lambda_{1,+}^* + 4D + i2\omega_0)$  and  $x_5(\omega_0) = (2\lambda_{1,+} + \lambda_{1,+}^* + D + i\omega_0)$ . In their terms, we may express the rest of the integrals, which read as

$$\mathcal{B}_{2,2} = \pi K_1^2 \mathcal{A}_{1,2} \mathcal{G}_+ \{ \mathbb{P}[x_1 x_4] + \mathbb{P}[x_1 x_4 x_5] \} + \pi K_1^2 c_3 \mathcal{G}_+ \{ \mathbb{P}[x_1^2 x_2 x_4] + \mathbb{P}[x_1^2 x_4 x_5] \} - \pi^3 K_1^4 \mathcal{G}_+ \{ \mathbb{P}[x_1^2 x_2 x_3 x_4] + \mathbb{P}[x_1^2 x_2 x_4 x_5] \} + K_2 \mathcal{A}_{2,2} \mathcal{G}_+ \mathbb{P}[x_1 x_4] + K_2 c_3 \mathcal{A}_{2,0} \mathcal{G}_+ \mathbb{P}[x_1 x_2 x_4] - \pi^2 K_1^2 K_2 \mathcal{A}_{2,0} \mathcal{G}_+ \{ \mathbb{P}[x_1^2 x_3 x_4] + \mathbb{P}[x_1 x_2 x_3 x_4] + \mathbb{P}[x_1 x_2 x_4 x_5] - \mathbb{P}[x_1 x_1^* x_4 x_5] \}, \quad (\text{SM14})$$

$$\mathcal{C}_{1,2}^* = \frac{K_1}{2} c_3 \mathcal{G}_+^* \mathbb{P}[x_1 x_1^* x_5] - \frac{\pi^2 K_1^3}{2} \mathcal{G}_+^* \mathbb{P}[x_1 x_1^* x_2 x_5] + \frac{\pi^2 K_1 K_2}{2} \mathcal{A}_{2,0} \mathcal{G}_+^* \left\{ \mathbb{P}[(x_1^*)^2 x_5] + \mathbb{P}[x_1^* x_2 x_5] \right\} + \frac{K_1}{2} \mathcal{A}_{1,2} \mathcal{G}_+^* \mathbb{P}[x_1^* x_5], \quad (\text{SM15})$$

$$\mathcal{B}_{3,0} = \frac{\pi^2 K_1^3}{2} \mathcal{G}_+ \mathbb{P}[x_1^2 x_2 x_3] + \frac{\pi K_1 K_2}{2} \mathcal{A}_{2,0} \mathcal{G}_+ \{ \mathbb{P}[x_1^2 x_3] + \mathbb{P}[x_1 x_2 x_3] \}. \quad (\text{SM16})$$

Putting all of these together into Eq. (SM53), we obtain  $c_5$ . Putting  $\omega_0 = 0$  into the final expression, we get back Eq. (SM8). From the definition of  $D_{\text{eff}}$ , we further get

$$D_{\text{eff}} = D \int_{-\infty}^{+\infty} d\omega' \left| \tilde{\psi}_1(\omega') \right|^2 g(\omega') = D \int_{-\infty}^{+\infty} d\omega' \left| \frac{\mathcal{G}_+^*}{(\lambda_{1,+}^* + D - i\omega')} \right|^2 g(\omega') = D |\mathcal{G}_+|^2 \mathcal{H}. \quad (\text{SM17})$$

For  $\alpha = 1/2$ , the case considered in the main text, many of these expressions simplify. Firstly, the eigenvalues of the operator  $\mathcal{L}$ , given by Eq. (SM3), simplify to

$$\lambda_{1,\pm} = -D + \frac{K_1}{4} \pm \sqrt{\left(\frac{K_1}{4}\right)^2 - \omega_0^2}. \quad (\text{SM18})$$

Now we are interested in determining the nature of transition at the transition point. In other words, we need to determine the sign of  $c_3$  at the transition point. At the transition point, we have  $\lambda_{1,+} = 0$ . Putting  $\lambda_{1,+} = 0$  and  $\alpha = 1/2$  into previously obtained expressions, we obtain

$$\begin{aligned} \mathcal{G}_+ &= \frac{2(D^2 + \omega_0^2)^2}{K_1(D^2 - \omega_0^2)}, \quad \mathcal{I} = \frac{2D^3 - 4\omega_0^2 D}{(D^2 + \omega_0^2)^2 (4D^2 + \omega_0^2)}, \quad \mathcal{A}_{2,0} = \frac{K_1^2}{2} \frac{2D^2 - \omega_0^2}{[D^2 + \omega_0^2] [4D^2 + \omega_0^2 - K_2 D]}, \\ \mathcal{H} &= \frac{2D^2 - \omega_0^2}{[4D^2 + \omega_0^2] [D^2 + \omega_0^2]}, \quad \mathcal{K} = \frac{1}{D^2 + \omega_0^2}. \end{aligned} \quad (\text{SM19})$$

Combining all of them, we obtain

$$c_3 = \frac{K_1^2 D}{(D^2 + \omega_0^2)^2 (4D^2 + \omega_0^2)} \frac{(2D^2 - 4\omega_0^2) (4D^2 + \omega_0^2) - DK_2 (4D^2 - 5\omega_0^2)}{4D^2 + \omega_0^2 - DK_2}. \quad (\text{SM20})$$

From the discussions and Figure 3(a) of the main text, the region of validity of our calculation with a two-dimensional unstable subspace is  $\omega_0 < D$  and  $K_2 < K_2^c = 4D + \omega_0^2/D$ . Hence, we have  $(4D^2 + \omega_0^2 - DK_2) > 0$  for the entire region of validity of our calculation. As a result, the sign of  $c_3$  will be determined from the sign of  $[(2D^2 - 4\omega_0^2) (4D^2 + \omega_0^2) - DK_2 (4D^2 - 5\omega_0^2)]$ . Hence, we may write

$$c_3 \propto [(2D^2 - 4\omega_0^2) (4D^2 + \omega_0^2) - DK_2 (4D^2 - 5\omega_0^2)]. \quad (\text{SM21})$$

The tri-critical point may be obtained from the condition  $c_3 = 0$ , which gives

$$\omega_0 = \frac{1}{2\sqrt{2}} \sqrt{5K_2 D - 14D^2 + D \sqrt{25K_2^2 - 204K_2 D + 324D^2}}. \quad (\text{SM22})$$

Equation (SM22) gives the black line in Figure (3) panel (b) of the main text separating the continuous and first-order transition regions.

Putting  $\alpha = 1/2$  in the expressions of  $\mathcal{G}_+$  and  $\mathcal{H}$  and putting them back in Eq. (SM17), we obtain

$$\begin{aligned} D_{\text{eff}} &= D |\mathcal{G}_+|^2 \mathcal{H} = D \left| \frac{2 [(\lambda_{1,+} + D)^2 + \omega_0^2]^2}{K_1 [(\lambda_{1,+} + D)^2 - \omega_0^2]} \right|^2 \frac{(\lambda_{1,+} + D) (\lambda_{1,+}^* + D) + \omega_0^2}{\left| [(\lambda_{1,+} + D)^2 + \omega_0^2] \right|^2} = D \frac{4 [(\lambda_{1,+} + D)^2 + \omega_0^2]^3}{[(\lambda_{1,+} + D)^2 - \omega_0^2]^2} \\ &= D \frac{4 \left[ \frac{K_1^2}{8} + \frac{K_1}{2} \sqrt{\frac{K_1^2}{16} - \omega_0^2} \right]^3}{\left[ \left( \frac{K_1}{4} + \sqrt{\left( \frac{K_1}{4} \right)^2 - \omega_0^2} \right)^2 - \omega_0^2 \right]^2}. \end{aligned} \quad (\text{SM23})$$

Hence, we have

$$D_{\text{eff}} \propto \left[ \left( \frac{K_1}{4} + \sqrt{\left( \frac{K_1}{4} \right)^2 - \omega_0^2} \right)^2 - \omega_0^2 \right]^{-2}, \quad (\text{SM24})$$

which diverges on the line  $K_1 = 4\omega_0$ .

### Appendix E: Results corresponding to the model in *Application 3* of the main text

In *Application 3: Stochastic Kuramoto model with harmonic and bi-harmonic interaction with Lorentzian frequency*, we consider

$$K_m = 0 \quad \forall m \geq 3, \text{ and } g(\omega) = \frac{\sigma}{\pi(\omega^2 + \sigma^2)}. \quad (\text{SM1})$$

Following Eq. (SM12), the spectral function becomes

$$\Lambda_m(x) = 1 - \frac{|m|K_{|m|}}{2(x + m^2D \pm m\sigma)}, \text{ if } \Re(x) \gtrless -m^2D, \text{ for } |m| = 1, 2. \quad (\text{SM2})$$

The roots of this spectral function give the eigenvalues, which read as

$$\lambda_m = |m|(K_m - 2\sigma)/2 - m^2D, \quad m = \pm 1, \pm 2 \quad (\text{SM3})$$

for  $K_m \geq 2\sigma$ . For  $m = \pm 1, \pm 2$  with  $K_m < 2\sigma$  and for  $m = \pm 3, \pm 4, \dots$ , the eigenvalues are  $\lambda_m = -m^2D - im\omega$ . Putting  $\sigma = 0$ , we get back the eigenvalues given in Eq. (SM3). Following Eq. (SM18), we have the eigenfunctions of  $L_m^\dagger$  for  $m = \pm 1, \pm 2$ , which read

$$\tilde{\psi}_m(\omega) = \frac{\mathcal{G}^*}{(\lambda_{m,\pm}^* + m^2D - im\omega)}, \quad \mathcal{G} = \frac{|m|K_{|m|}}{2}. \quad (\text{SM4})$$

Evaluating the relevant expressions in Eq. (SM52), we obtain

$$\mathcal{C}_{1,0} = \frac{K_1}{K_1 - 2\sigma}, \quad \mathcal{A}_{2,0} = \mathcal{B}_{2,0} = \frac{2\pi K_1}{K_1 - K_2 + 2D}. \quad (\text{SM5})$$

Using these expressions, we obtain  $c_3$  from Eq. (SM52), which reads as

$$c_3 = \frac{2\pi^2 K_1^2}{K_1 - 2\sigma} \left( \frac{K_1 - K_2 - 2\sigma}{K_1 - K_2 + 2D} \right). \quad (\text{SM6})$$

Using the expression of  $c_3$ , we further compute

$$\begin{aligned} \mathcal{A}_{1,2} &= -\frac{2\pi^2 \sigma K_1 [K_1^3 - 2K_1 K_2 (2D + \sigma) + 4K_2 (D + \sigma) (3D + 2\sigma) - K_1^2 (K_2 + 2\sigma)]}{(K_1 - K_2 + 2D)(K_1 - 2\sigma)(K_1 - 2D - 2\sigma)(K_1 - 3D - 2\sigma)(K_1 - 2D - 4\sigma)}, \text{ if } \left(2\sigma + \frac{4}{3}D\right) > K_1 > 2\sigma, \\ &= -\frac{2\pi^2 \sigma K_1 K_2}{(K_1 - K_2 + 2D)(K_1 - 2\sigma)(K_1 - D - 2\sigma)}, \text{ if } K_1 > \left(2\sigma + \frac{4}{3}D\right). \end{aligned} \quad (\text{SM7})$$



In this model, the transition point is  $K_1^c = 2(D + \sigma)$ . Since  $K_1^c > 2\sigma + 4D/3$  and we are mostly interested in the finite-size fluctuations near the transition point, here we compute the rest of the expressions for  $K_1 > (2\sigma + 4D/3)$ . They read as

$$\begin{aligned} \mathcal{A}_{2,2} &= \frac{2K_1^2\pi^2\mathcal{E}_1}{3(4D_0 + K_1)(2D_0 + K_1 - K_2)^2(K_1 - 2\sigma)(-D_0 + K_1 - 2\sigma)(K_1 - \sigma)}, \text{ where} \\ \mathcal{E}_1 &= 6K_1(-D_0 + K_1)(2D_0K_1 - (6D_0 + K_1)K_2 + K_2^2)\pi + 4(6D_0(D_0 - 2K_1)K_1 \\ &\quad + 2(-7D_0^2 + 9D_0K_1 + K_1^2)K_2 + (7D_0 - 5K_1)K_2^2)\pi\sigma + 24(2D_0(K_1 - K_2) + K_2^2)\pi\sigma^2 \end{aligned} \quad (\text{SM8})$$

$$\mathcal{C}_{1,2}^* = -\frac{K_1\pi^2\sigma[-D_0K_1(K_1 - 2K_2)(K_1 - 2\sigma) + 4D_0^2K_2(-K_1 + \sigma) + (K_1 - 2\sigma)^2(K_1^2 + 4K_1K_2 - 4K_2\sigma)]}{(2D_0 + K_1 - K_2)(K_1 - 2\sigma)^2(-D_0 + K_1 - 2\sigma)^2(D_0 + K_1 - 2\sigma)}, \quad (\text{SM9})$$

$$\begin{aligned} \mathcal{B}_{2,2} &= \frac{4K_1^2\pi^3\mathcal{E}_2}{3(4D_0 + K_1)(2D_0 + K_1 - K_2)^2(K_1 - 2\sigma)^2(-D_0 + K_1 - 2\sigma)(2K_1 - K_2 - 2\sigma)}, \text{ where} \\ \mathcal{E}_2 &= 6K_1^2(-D_0 + K_1)(2D_0K_1 - (6D_0 + K_1)K_2 + K_2^2) + (24D_0(2D_0 - 3K_1)K_1^2 + 2K_1(-56D_0^2 + 72D_0K_1 \\ &\quad + 11K_1^2)K_2 + (-8D_0^2 + 26D_0K_1 - 35K_1^2)K_2^2 + (4D_0 + K_1)K_2^3)\sigma - 6(8D_0^2(K_1 - 2K_2) + K_1(3K_1 - 11K_2)K_2 \\ &\quad + D_0(-24K_1^2 + 34K_1K_2 + 8K_2^2))\sigma^2 - 48(2D_0(K_1 - K_2) + K_2^2)\sigma^3, \end{aligned} \quad (\text{SM10})$$

$$\mathcal{B}_{3,0} = \frac{4\pi^2K_1(K_1 + K_2)}{(K_1 + 4D)(K_1 - K_2 + 2D)}. \quad (\text{SM11})$$

Putting all of these together into Eq. (SM53), we obtain  $c_5$ .

From the definition of  $D_{\text{eff}}$ , we further get

$$D_{\text{eff}} = D \int_{-\infty}^{+\infty} d\omega' \left| \tilde{\psi}_1(\omega') \right|^2 g(\omega') = \frac{DK_1}{K_1 - 2\sigma}. \quad (\text{SM12})$$

#### Appendix F: Derivation of Eq. (13)

For the model in *Application 1*, we have  $g(\omega) = \delta(\omega)$ ,  $\lambda_1 = K_1/2 - D$  and

$$\Lambda_1'(x) = \frac{K_1}{2(x + D)^2}, \quad (\text{SM1})$$

which immediately gives  $\Lambda_1'(\lambda_1) = 2/K_1$ . Hence, we further get  $\psi_1 = \delta(\omega)$  and

$$\tilde{\psi}_1(\omega) = \frac{1}{[\Lambda_1'(\lambda_1)]^*} \frac{1}{(\lambda_1^* + D - i\omega)} = \frac{K_1}{K_1 - i2\omega}. \quad (\text{SM2})$$

Another relevant quantity for this calculation is

$$w_{2,0}(\omega) = \frac{\pi K_1 \psi_1(\omega)}{(\lambda_1 + 2D + i\omega)} = \frac{2\pi K_1 \delta(\omega)}{(K_1 + 2D)}. \quad (\text{SM3})$$

Let us now start from Eq. (SM28). We have

$$\dot{A}(t) = \left( \tilde{\Psi}_1, \mathcal{L}\eta \right) + \left( \tilde{\Psi}_1, \mathcal{N}[\eta] \right) + \left( \tilde{\Psi}_1, \sqrt{\frac{2D}{N}} \frac{\partial}{\partial \theta} \left[ \sqrt{\frac{\delta(\omega)}{2\pi} + \eta(\theta, \omega, t)} \zeta(\theta, \omega, t) \right] \right). \quad (\text{SM4})$$

We have computed in Section A the first two terms, which become  $\lambda_1 A$  and  $-c_3 A|A|^2$  (in the leading order), respectively, where  $c_3$  is given by Eq. (SM6). Defining the third term as noise  $\mathbf{N}(t)$ , we have

$$\begin{aligned} \mathbf{N}(t) &= \frac{1}{2\pi} \sqrt{\frac{2D}{N}} \int_{-\infty}^{\infty} d\omega \int_0^{2\pi} d\theta \tilde{\psi}_1^*(\omega) e^{-i\theta} \frac{\partial}{\partial \theta} \left[ \sqrt{\frac{\delta(\omega)}{2\pi} + \eta(\theta, \omega, t)} \zeta(\theta, \omega, t) \right] \\ &= \frac{i}{2\pi} \sqrt{\frac{2D}{N}} \int_{-\infty}^{\infty} d\omega \int_0^{2\pi} d\theta \tilde{\psi}_1^*(\omega) e^{-i\theta} \sqrt{\frac{\delta(\omega)}{2\pi} + \eta(\theta, \omega, t)} \zeta(\theta, \omega, t), \end{aligned} \quad (\text{SM5})$$

where we have performed integration by parts. Let us compute the properties of the noise. Clearly, we have  $\langle \mathbf{N}(t) \rangle = 0$ . Now, we have

$$\begin{aligned}
& \langle \mathbf{N}(t) \mathbf{N}(t') \rangle \\
&= -\frac{D}{2\pi^2 N} \int d\omega d\omega' d\theta d\theta' \tilde{\psi}_1^*(\omega) \tilde{\psi}_1^*(\omega') e^{-i(\theta+\theta')} \sqrt{\left[ \frac{\delta(\omega)}{2\pi} + \eta(\theta, \omega, t) \right] \left[ \frac{\delta(\omega')}{2\pi} + \eta(\theta', \omega', t') \right]} \langle \zeta(\theta, \omega, t) \zeta(\theta', \omega', t') \rangle \\
&= -\frac{D}{2\pi^2 N} \int d\omega d\omega' d\theta d\theta' \tilde{\psi}_1^*(\omega) \tilde{\psi}_1^*(\omega') e^{-i(\theta+\theta')} \sqrt{\left[ \frac{\delta(\omega)}{2\pi} + \eta(\theta, \omega, t) \right] \left[ \frac{\delta(\omega')}{2\pi} + \eta(\theta', \omega', t') \right]} \delta(\theta - \theta') \delta(\omega - \omega') \delta(t - t') \\
&= -\delta(t - t') \frac{D}{2\pi^2 N} \int_{-\infty}^{\infty} d\omega \int_0^{2\pi} d\theta \left[ \tilde{\psi}_1^*(\omega') \right]^2 e^{-i2\theta} \left[ \frac{\delta(\omega)}{2\pi} + \eta(\theta, \omega, t) \right] \tag{SM6} \\
&= -\delta(t - t') \frac{D}{2\pi^2 N} \int_{-\infty}^{\infty} d\omega \left[ \tilde{\psi}_1^*(\omega') \right]^2 \int_0^{2\pi} d\theta e^{-i2\theta} \eta(\theta, \omega, t), \tag{SM7}
\end{aligned}$$

where we have used  $\int_0^{2\pi} d\theta e^{-i2\theta} = 0$ . Using the Fourier expansion of  $\eta$ , we obtain

$$\langle \mathbf{N}(t) \mathbf{N}(t') \rangle = -\delta(t - t') \frac{D}{\pi N} \int_{-\infty}^{\infty} d\omega \left[ \tilde{\psi}_1^*(\omega') \right]^2 W_2[A, A^*] = -\delta(t - t') \frac{DA^2}{\pi N} \int_{-\infty}^{\infty} d\omega \left[ \tilde{\psi}_1^*(\omega') \right]^2 w_{2,0}(\omega) + \mathcal{O}(A^2|A|^2). \tag{SM8}$$

Now, putting the expressions of  $\tilde{\psi}_1(\omega)$  and  $w_{2,0}(\omega)$ , we obtain

$$\int_{-\infty}^{\infty} d\omega \left[ \tilde{\psi}_1^*(\omega') \right]^2 w_{2,0}(\omega) = \int_{-\infty}^{\infty} d\omega \left[ \frac{K_1}{K_1 + i2\omega} \right]^2 \frac{2\pi K_1 \delta(\omega)}{(K_1 + 2D)} = \frac{2\pi K_1}{(K_1 + 2D)}. \tag{SM9}$$

Hence, in the leading order, we have

$$\langle \mathbf{N}(t) \mathbf{N}(t') \rangle = -\frac{A^2}{N} \left[ \frac{2K_1 D}{K_1 + 2D} \right] \delta(t - t'). \tag{SM10}$$

In a similar way, we compute

$$\begin{aligned}
& \langle \mathbf{N}(t) \mathbf{N}^*(t') \rangle \\
&= \frac{D}{2\pi^2 N} \int d\omega d\omega' d\theta d\theta' \tilde{\psi}_1^*(\omega) \tilde{\psi}_1(\omega') e^{-i(\theta-\theta')} \sqrt{\left[ \frac{\delta(\omega)}{2\pi} + \eta(\theta, \omega, t) \right] \left[ \frac{\delta(\omega')}{2\pi} + \eta(\theta', \omega', t) \right]} \langle \zeta(\theta, \omega, t) \zeta(\theta', \omega', t') \rangle \\
&= \frac{D}{2\pi^2 N} \int d\omega d\omega' d\theta d\theta' \tilde{\psi}_1^*(\omega) \tilde{\psi}_1(\omega') e^{-i(\theta-\theta')} \sqrt{\left[ \frac{\delta(\omega)}{2\pi} + \eta(\theta, \omega, t) \right] \left[ \frac{\delta(\omega')}{2\pi} + \eta(\theta', \omega', t) \right]} \delta(\theta - \theta') \delta(\omega - \omega') \delta(t - t') \\
&= \delta(t - t') \frac{D}{2\pi^2 N} \int_{-\infty}^{\infty} d\omega \int_0^{2\pi} d\theta \left| \tilde{\psi}_1(\omega') \right|^2 \left[ \frac{\delta(\omega)}{2\pi} + \eta(\theta, \omega, t) \right] \tag{SM11} \\
&= \delta(t - t') \frac{D}{2\pi^2 N} \left[ \int_{-\infty}^{\infty} d\omega \left| \tilde{\psi}_1(\omega') \right|^2 \delta(\omega) \right] \left[ \frac{1}{2\pi} \int_0^{2\pi} d\theta \right]. \tag{SM12}
\end{aligned}$$

Hence, we have

$$\langle \mathbf{N}(t) \mathbf{N}^*(t') \rangle = \left[ \frac{D}{2\pi^2 N} \right] \delta(t - t'), \tag{SM13}$$

The equation for  $A$  is then

$$dA = (\lambda_1 A - c_3 A |A|^2) dt + d\mathbf{N}(t), \tag{SM14}$$

where the complex noise  $\mathbf{N}$  is gaussian, centered, and determined by its correlations (SM10) and (SM13).

Now, we want to compute the evolution of  $r = |A| = \sqrt{AA^*}$ ; this requires the use of Ito formula. For the sake of complete-

ness, we give the whole computation. Taylor expansion up to the second order gives

$$dr = \frac{\partial r}{\partial A} dA + \frac{\partial r}{\partial A^*} dA^* + \frac{1}{2} \left[ \frac{\partial^2 r}{\partial A \partial A} dA dA + 2 \frac{\partial^2 r}{\partial A^* \partial A} dA^* dA + \frac{\partial^2 r}{\partial A^* \partial A^*} dA^* dA^* \right]. \quad (\text{SM15})$$

Now, we have

$$\frac{\partial r}{\partial A} = \frac{A^*}{2r}, \quad \frac{\partial r}{\partial A^*} = \frac{A}{2r}, \quad \frac{\partial^2 r}{\partial A \partial A} = -\frac{r}{4A^2}, \quad \frac{\partial^2 r}{\partial A^* \partial A} = \frac{\partial^2 r}{\partial A \partial A^*} = \frac{1}{4r}, \quad \frac{\partial^2 r}{\partial A^* \partial A^*} = -\frac{r}{4(A^*)^2}. \quad (\text{SM16})$$

Considering terms up to  $\mathcal{O}(dt)$ , and using (SM10) and (SM13), we obtain

$$\begin{aligned} dr &= \frac{A^*}{2r} [(\lambda_1 A - c_3 A |A|^2) dt + d\mathbf{N}(t)] + \frac{A}{2r} [(\lambda_1 A^* - c_3 A^* |A|^2) dt + d\mathbf{N}^*(t)] \\ &\quad + \frac{1}{2} \left[ \frac{r}{4A^2} \frac{A^2}{N} \left[ \frac{2K_1 D}{K_1 + 2D} \right] + 2 \frac{1}{4r} \left[ \frac{D}{2\pi^2 N} \right] + \frac{r}{4(A^*)^2} \frac{(A^*)^2}{N} \left[ \frac{2K_1 D}{K_1 + 2D} \right] \right] dt \end{aligned} \quad (\text{SM17})$$

$$= \left\{ \lambda_1 r - c_3 r^3 + \frac{D}{8\pi^2 N r} \left[ 1 + r^2 \left( \frac{4\pi^2 K_1}{K_1 + 2D} \right) \right] \right\} dt + \frac{1}{2r} [A^* d\mathbf{N}(t) + A d\mathbf{N}^*(t)], \quad (\text{SM18})$$

which gives

$$\frac{dr}{dt} = \lambda_1 r - c_3 r^3 + \frac{D}{8\pi^2 N r} \left[ 1 + r^2 \left( \frac{4\pi^2 K_1}{K_1 + 2D} \right) \right] + \mathbf{N}_r(t), \quad (\text{SM19})$$

where  $\mathbf{N}_r(t) = (2r)^{-1} [A^* \mathbf{N}(t) + A \mathbf{N}^*(t)]$ . Since  $A(t)$  and  $\mathbf{N}(t)$  are independent, the correlation properties of the gaussian noise  $N_r$  can be obtained from (SM10) and (SM13); we obtain

$$\langle \mathbf{N}_r(t) \rangle = 0, \quad \langle \mathbf{N}_r(t) \mathbf{N}_r(t') \rangle = \frac{D}{4\pi^2 N} \left[ 1 - r^2 \left( \frac{4\pi^2 K_1}{K_1 + 2D} \right) \right] \delta(t - t'). \quad (\text{SM20})$$

Hence, we may write

$$\mathbf{N}_r(t) = \sqrt{\frac{D}{4\pi^2 N} \left[ 1 - r^2 \left( \frac{4\pi^2 K_1}{K_1 + 2D} \right) \right]} \xi_r(t), \quad (\text{SM21})$$

where we have  $\langle \xi_r(t) \rangle = 0$  and  $\langle \xi_r(t) \xi_r(t') \rangle = \delta(t - t')$ . Hence, we get

$$\frac{dr}{dt} = \lambda_1 r - c_3 r^3 + \frac{D}{8\pi^2 N r} \left[ 1 + r^2 \left( \frac{4\pi^2 K_1}{K_1 + 2D} \right) \right] + \sqrt{\frac{D}{4\pi^2 N} \left[ 1 - r^2 \left( \frac{4\pi^2 K_1}{K_1 + 2D} \right) \right]} \xi_r(t). \quad (\text{SM22})$$

Substituting  $r = R_1/(2\pi)$ , we obtain

$$\frac{dR_1}{dt} = \lambda_1 R_1 - \frac{c_3}{4\pi^2} R_1^3 + \frac{D}{2N R_1} \left[ 1 + R_1^2 \left( \frac{K_1}{K_1 + 2D} \right) \right] + \sqrt{\frac{D}{N} \left[ 1 - R_1^2 \left( \frac{K_1}{K_1 + 2D} \right) \right]} \xi_r(t). \quad (\text{SM23})$$

The above is Eq. (13) of the main text.